J Arid Land 2024 16(10): 1380–1408
doi: 10.1007/s40333-024-0062-7; CSTR: 32276.14.JAL.02400627

Science Press Springer-Verlag

Predicting changes in the suitable habitats of six halophytic plant species in the arid areas of Northwest China

YANG Ao[1,2,3,4], TU Wenqin[5], YIN Benfeng[2,3,4], ZHANG Shujun[2,3,4,6], ZHANG Xinyu[7], ZHANG Qing[2,3,4,8], HUANG Yunjie[2,3,4,6], HAN Zhili[2,3,4,9], YANG Ziyue[1,2,3,10], ZHOU Xiaobing[2,3,4], ZHUANG Weiwei[1*], ZHANG Yuanming[2,3,4]

[1] College of Life Sciences, Xinjiang Normal University/Xinjiang Key Laboratory of Special Species Conservation and Regulatory Biology/Key Laboratory of Special Environment Biodiversity Application and Regulation in Xinjiang/Key Laboratory of Plant Stress Biology in Arid Land, Urumqi 830054, China;
[2] State Key Laboratory of Desert and Oasis Ecology, Key Laboratory of Ecological Safety and Sustainable Development in Arid Lands, Xinjiang Institute of Ecology and Geography, Chinese Academy of Sciences, Urumqi 830011, China;
[3] Xinjiang Key Laboratory of Biodiversity Conservation and Application in Arid Lands, Xinjiang Institute of Ecology and Geography, Chinese Academy of Sciences, Urumqi 830011, China;
[4] Xinjiang Field Scientific Observation Research Station of Tianshan Wild Fruit Forest Ecosystem, Yili Botanical Garden, Xinjiang Institute of Ecology and Geography, Chinese Academy of Sciences, Xinyuan 835800, China;
[5] State Key Laboratory of Earth Surface Processes and Resource Ecology, College of Life Sciences, Beijing Normal University, Beijing 100875, China;
[6] University of Chinese Academy of Sciences, Beijing 100049, China;
[7] College of Biological Sciences, University of California Davis, Davis, CA 95616, USA;
[8] College of Ecology and Environment, Xinjiang University, Urumqi 830017, China;
[9] College of Resources and Environment/Xinjiang Key Laboratory of Soil and Plant Ecological Processes, Xinjiang Agricultural University, Urumqi 830052, China;
[10] College of Grassland Science, Xinjiang Agricultural University, Urumqi 830052, China

Abstract: In the context of changes in global climate and land uses, biodiversity patterns and plant species distributions have been significantly affected. Soil salinization is a growing problem, particularly in the arid areas of Northwest China. Halophytes are ideal for restoring soil salinization because of their adaptability to salt stress. In this study, we collected the current and future bioclimatic data released by the WorldClim database, along with soil data from the Harmonized World Soil Database (v1.2) and A Big Earth Data Platform for Three Poles. Using the maximum entropy (MaxEnt) model, the potential suitable habitats of six halophytic plant species (*Halostachys caspica* (Bieb.) C. A. Mey., *Halogeton glomeratus* (Bieb.) C. A. Mey., *Kalidium foliatum* (Pall.) Moq., *Halocnemum strobilaceum* (Pall.) Bieb., *Salicornia europaea* L., and *Suaeda salsa* (L.) Pall.) were assessed under the current climate conditions (average for 1970–2000) and future (2050s, 2070s, and 2090s) climate scenarios (SSP245 and SSP585, where SSP is the Shared Socio-economic Pathway). The results revealed that all six halophytic plant species exhibited the area under the receiver operating characteristic curve values higher than 0.80 based on the MaxEnt model, indicating the excellent performance of the MaxEnt model. The suitability of the six halophytic plant species significantly varied across regions in the arid areas of Northwest China. Under different future climate change scenarios, the suitable habitat areas for the six halophytic plant species are expected to increase or decrease to varying degrees. As global warming progresses, the suitable habitat areas of *K. foliatum*, *S. salsa*, and *H. strobilaceum* exhibited an increasing trend. In contrast, the suitable habitat areas of *H. glomeratus*, *S. europaea*, and *H. caspica* showed an opposite trend. Furthermore, considering the ongoing global warming trend, the

*Corresponding author: ZHUANG Weiwei (E-mail: zww8611@sina.com)
The first, second, and third authors contributed equally to this work.
Received 2024-03-18; revised 2024-07-07; accepted 2024-07-23

centroids of the suitable habitat areas for various halophytic plant species would migrate to different degrees, and four halophytic plant species, namely, *S. salsa*, *H. strobilaceum*, *H. glomeratus*, and *H. capsica*, would migrate to higher latitudes. Temperature, precipitation, and soil factors affected the possible distribution ranges of these six halophytic plant species. Among them, precipitation seasonality (coefficient of variation), precipitation of the warmest quarter, mean temperature of the warmest quarter, and exchangeable Na^+ significantly affected the distribution of halophytic plant species. Our findings are critical to comprehending and predicting the impact of climate change on ecosystems. The findings of this study hold significant theoretical and practical implications for the management of soil salinization and for the utilization, protection, and management of halophytes in the arid areas of Northwest China.

Keywords: halophytes; climate change; global warming; maximum entropy (MaxEnt) model; soil salinization; suitable habitats; Northwest China

Citation: YANG Ao, TU Wenqin, YIN Benfeng, ZHANG Shujun, ZHANG Xinyu, ZHANG Qing, HUANG Yunjie, HAN Zhili, YANG Ziyue, ZHOU Xiaobing, ZHUANG Weiwei, ZHANG Yuanming. 2024. Predicting changes in the suitable habitats of six halophytic plant species in the arid areas of Northwest China. Journal of Arid Land, 16(10): 1380–1408. https://doi.org/10.1007/s40333-024-0062-7; https://cstr.cn/32276.14.JAL.02400627

1 Introduction

Global climate change and land use change are recognized as the primary factors leading to the global decline in biodiversity (Barbet-Massin et al., 2012; Pimm et al., 2014). These changes lead to ecosystem degradation; species gradually lose their suitable habitats, thus threatening biodiversity (Ceballos et al., 2015; Warren et al., 2018; Román-Palacios and Wiens, 2020). Currently, approximately 25.00% of the species are threatened with extinction due to climate change. Since plants are more vulnerable to environmental changes than animals (IPBES, 2019), climate change significantly impacts the extinction and spread of plant species (Grant and Grant, 2002; Thomas et al., 2006; Foden et al., 2007; Pías et al., 2010; Mantyka-Pringle et al., 2015). This is evidenced by the rapid decline in plant species observed in regions such as the Qinghai-Xizang Plateau, China (Klein et al., 2004) and the salt marshes of New England in the United States (Gedan and Bertness, 2009). Extensive experiments conducted at Cedar Creek in the United States revealed that the reduction in plant species richness can result in decreased ecosystem stability (Hautier et al., 2015). Considering global warming, predicting the potential suitable habitats of plant species has become critical in ecological, biogeographical, and global biological studies. The prediction of species distribution trends under global climate change is crucial for analyzing potential species distribution and planning strategies for species protection and sustainable resource utilization (Liu et al., 2018; Lu et al., 2021b).

The species distribution model (SDM) uses statistical or biophysical methods to link the records of locations of species occurrence to environmental factors on a range of time and spatial scales. Therefore, this model is a convenient tool to evaluate how climate change may affect the biodiversity and potential patterns of species distribution in the future (Hirzel et al., 2002; Elith and Leathwick, 2009; Foden et al., 2019; Feeley et al., 2020). With the rapid development of 3S technology (geographic information system (GIS), remote sensing (RS), and global positioning system (GPS)), various models have been developed to assess the suitable habitats of species. Currently, there are approximately 14 different SDMs, and the following models are most often used: random forest (Cutler et al., 2007), genetic algorithm for rule-set prediction (Stockwell, 1999), growth regression tree model (Elith et al., 2008), Bioclim (Beaumont et al., 2005), and maximum entropy (MaxEnt) (Elith et al., 2006). The MaxEnt model is widely used because of its high prediction precision and fast processing speed (Phillips et al., 2006). This model has exhibited significant advances; it is used for conserving treasured animals and plants (Yi et al., 2016; Yang et al., 2020, 2021), assessing the risk of invasive species (Tu et al., 2021; Zhang et al., 2021), and protecting the maritime environment (Mamun et al., 2018; Melo-Merino et al., 2020).

Soil salinization has become an ecological problem worldwide, affecting soil resources (Hassani et al., 2021). The total worldwide area of saline–alkali land is approximately 100.00×10^6

km^2 (Khan et al., 2020; Hopmans et al., 2021), of which 20.00% is irrigated land (Liu and Wang, 2021). In China, the saline–alkali land area is 0.99×10^6 km^2 (Liu et al., 2019, 2024), which is mainly distributed in Northwest China, North China, Northeast China, and coastal areas (Liu et al., 2024). Current methods to manage soil salinization, particularly in arid and semi-arid areas, have been facing significant challenges. Research is ongoing to improve these methods (Hassani et al., 2021; Singh, 2021; Zhao et al., 2024). Soil salinization can significantly impact vegetation growth, soil quality, and crop yields (Ma et al., 2018; Wang et al., 2018). Therefore, developing a plan for using and managing saline–alkaline land is crucial to address the issues of food security and scarcity of arable land.

Based on the causes and characteristics of local soil salinization, many countries and regions worldwide have developed various strategies to improve the utilization of saline–alkaline land (Li et al., 2005). The current methods for managing and improving saline–alkaline land primarily involve physical, chemical, and biological techniques including selecting appropriate irrigation method, leveling the land, planting salt-tolerant species, applying materials such as gypsum, and even adopting some extensive technical measures (Hammer et al., 2011; Han et al., 2013; Zhao et al., 2016). Among them, plantation of halophytes is a superior method because of their significant economic benefit and sustainability (Guo et al., 2022; Wang et al., 2023).

Halophytes are ideal candidates for the remediation and improvement of saline–alkaline soil (Shabala, 2013; Hasanuzzaman et al., 2014; Nouri et al., 2017), because they are able to endure and procreate in conditions where the salt content is 200 mmol/L NaCl or more (Flowers and Colmer, 2008). Halophytes can effectively ameliorate saline–alkaline soil because of their co-evolution with the saline soil environment (Zhang and Shi, 2013; Shabala et al., 2014). Halophytes can be categorized into enhalophytes, pseudo-halophytes, and recretohalophytes based on their salt tolerance mechanisms (Flowers et al., 2010; Shao et al., 2014). These plants exhibit various physiological and morphological features to counteract salt stress, such as actively expelling ions, regulating microclimate, reducing water evaporation, inhibiting soil salinity increase, and preventing soil salinization (Rabhi et al., 2009; Jesus et al., 2015; Ahmadi et al., 2022). At the same time, halophytes can increase soil organic matter, improve soil fertility, and neutralize soil alkalinity after the degradation of their roots, stems, and leaves in soil (Fang et al., 2014). Significant progress is seen in recent decades in terms of understanding the salt tolerance mechanisms of halophytic plant species (Ahanger et al., 2020; Hamani et al., 2020; Ju et al., 2023); however, most studies have mainly focused on the seedling breeding and tissue culture techniques of halophytes to assess their salt tolerance and genetic diversity (Yuan et al., 2020; Llanes et al., 2021; Zhou et al., 2024). The research predicting the geographical distribution of halophytes has mostly focused on the changes in the suitable habitats and influencing factors in coastal wetlands (Cao et al., 2022). However, reports on the probable distribution of halophytes in arid areas remain scarce.

Therefore, in this study, we explored the distribution patterns of six typical halophytic plant species widely distributed in arid areas, including *Halostachys caspica* (Bieb.) C. A. Mey., *Halogeton glomeratus* (Bieb.) C. A. Mey., *Kalidium foliatum* (Pall.) Moq., *Halocnemum strobilaceum* (Pall.) Bieb., *Salicornia europaea* L., and *Suaeda salsa* (L.) Pall., and determined the environmental factors influencing their habitat suitability. Using the MaxEnt model combined with GIS tools, we evaluated the potential suitable ranges and changes in the habitats of these halophytic plant species under different climate scenarios. The aims of this study were: (1) to investigate the potential suitable distribution ranges of six halophytic plant species (*H. glomeratus*, *H. capsica*, *K. foliatum*, *H. strobilaceum*, *S. europaea*, and *S. salsa*) and explore the important ecological factors affecting the potential distribution of these plant species in the arid areas of Northwest China in the current period; (2) to model the possible habitat ranges of these halophytic plant species in the future (2050s, 2070s, and 2090s), considering two Shared Socio-economic Pathways (SSPs), namely, SSP245 and SSP585; and (3) to assess the dynamic changes in the distribution and habitat suitability of these halophytic plant species under future climate scenarios. The study can provide scientific support for restoring, preserving, and

managing saline–alkaline land ecosystems and coordinating the sustainable development, utilization, and conservation of halophytes in the arid areas of Northwest China.

2 Materials and methods

2.1 Study area

The study area, located between 31°42′–53°23′N and 73°40′–126°04′E, covers six provinces and autonomous regions in Northwest China, i.e., Xinjiang Uygur Autonomous Region (Xinjiang), Gansu Province (Gansu), Qinghai Province (Qinghai), Shaanxi Province (Shaanxi), Ningxia Hui Autonomous Region (Ningxia), and Inner Mongolia Autonomous Region (Inner Mongolia) (Fig. 1). Topography of this region is predominated by plateaus, mountains, and basins. This region has the widest expanse of saline–alkaline land in China, notably in Xinjiang, Qaidam Basin of Qinghai, Hexi Corridor of Gansu, and western Inner Mongolia (Wang et al., 2021). Situated in the northwestern inland area of China, the region is characterized by the arid and semi-arid climate. The average annual temperature ranges from 0.00°C to 16.00°C, with a trend of increasing from northeast to southwest. The annual precipitation is under 200.00 mm in arid areas; whereas in semi-arid areas, it ranges from 200.00 to 400.00 mm, decreasing gradually from east to west. Due to the significant disparity between evaporation and precipitation throughout the year and unreasonable agriculture irrigation methods utilized in the study area, salt accumulation occurs on the ground surface, which results in serious soil salinization.

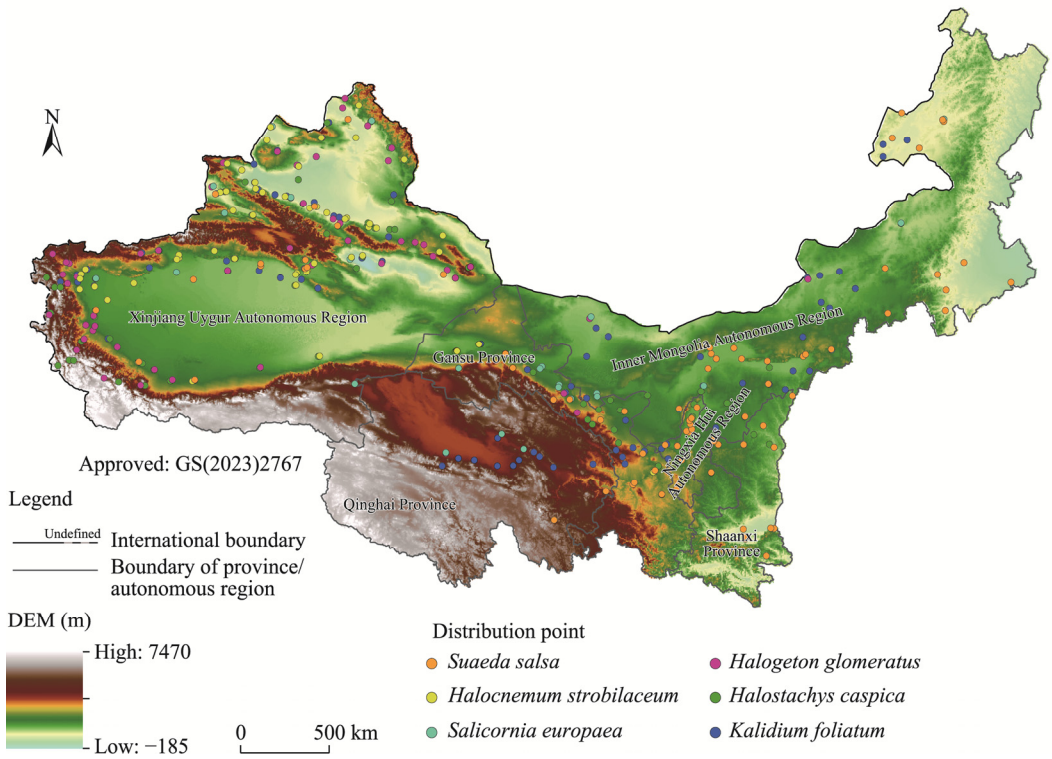

Fig. 1 Overview of the study area based on the digital elevation model (DEM) and distribution points of six halophytic plant species (*Halostachys caspica* (Bieb.) C. A. Mey., *Halogeton glomeratus* (Bieb.) C. A. Mey., *Kalidium foliatum* (Pall.) Moq., *Halocnemum strobilaceum* (Pall.) Bieb., *Salicornia europaea* L., and *Suaeda salsa* (L.) Pall.) in the arid areas of Northwest China. The DEM data were obtained from the Hydrological data and maps based on SHuttle Elevation Derivatives at multiple Scales (HydroSHEDS; https://hydrosheds.org/downloads). Note that the figure is based on the standard map (GS(2023)2767) of the Map Service System (http://bzdt.ch.mnr.gov.cn/) marked by the Ministry of Natural Resources of the People's Republic of China, and the boundary of the standard map has not been modified.

2.2 Occurrence of six halophytic plant species

In addition to field surveys of the selected six halophytic plant species in this study during June–September in 2023, occurrence information was collected from the Chinese Virtual Herbarium (http://www.cvh.org.cn), Specimen Resources Sharing Platform for Education (http://nh.scu.edu.cn/list/locality), Global Biodiversity Information Facility (http://www.gbif.org), and National Specimen Information Infrastructure (http://www.sii.org.cn/). A total of 1432 geographical distribution points were obtained for the six halophytic plant species (427 for *S. salsa*, 111 for *S. europaea*, 307 for *K. foliatum*, 286 for *H. caspica*, 151 for *H. glomeratus*, and 150 for *H. strobilaceum*). We removed the duplicate and unclear records according to the software requirements for building an SDM. To reduce the impact of sampling deviation on model accuracy (Warren et al., 2010), we used the ENMTools software (https://github.com/danlwarren/ENMTools) to trim the distribution points. Finally, 645 geographical distribution points were selected (77 for *S. salsa*, 69 for *S. europaea*, 167 for *K. foliatum*, 167 for *H. caspica*, 99 for *H. glomeratus*, and 66 for *H. strobilaceum*). The species distribution point format was converted into ".csv" format to ensure that the model can run smoothly (Li et al., 2020). Importantly, the accuracy of the MaxEnt modeling findings employed in this study was unaffected by fluctuations in occurrence data (Xiong et al., 2019; Fang et al., 2021). ArcGIS 10.8 (ESRI) was used to build the grids (1 km×1 km for each) in the study area, ensuring only one record in each grid (Fig. 1).

2.3 Environmental variables and processing

In this study, 40 environmental variables were selected to construct the MaxEnt model, including 19 bioclimatic factors, 3 topographic factors, and 18 soil factors (Table S1). The 19 bioclimatic and altitude factors were collected from WorldClim (http ://www.worldclim.org/). The slope and aspect data were calculated using the slope and aspect tools in ArcGIS 10.8 software. The WorldClim dataset provides version 2.1 of bioclimatic data with a spatial resolution of 2.5′, covering the period from 1970 to 2000, as well as future bioclimatic data (note that the bioclimatic data in the 2050s, 2070s, and 2090s represent the average values during the periods of 2041–2060, 2061–2080, and 2081–2100, respectively). We employed predictions from a high-resolution version of the Beijing Climate Center Climate System Model (Zhao et al., 2021), which is part of the Coupled Model Intercomparison Project Phase 6 conducted by the Intergovernmental Panel on Climate Change (IPCC) (Popp et al., 2017). The predictions were based on the scenarios of SSPs reflecting future climate change, indicating that the model is well-suited for studies in China (Yang et al., 2016; Wu et al., 2019). In accordance with the Sixth Assessment Report of the IPCC published in 2021 (Lynn and Peeva, 2021), SSP245 and SSP585 respectively indicate the moderate and highest forcing scenarios (radiative forcing 4.5 and 8.5 W/m^2 in 2100, respectively) (Thomson et al., 2011; Xian et al., 2022). The soil factor data were obtained from the Harmonized World Soil Database v1.2 (https://www.fao.org/) (FAO, 2012), and A Big Earth Data Platform for Three Poles (https://poles.tpdc.ac.cn/) was used to download Chinese soil organic matter data with a resolution of 1 km (Wei et al., 2013). All the above 40 environmental variables are listed in Table S1. Finally, using ArcGIS 10.8 Conversion tools, all environmental variables were converted to "ASCII" format, and their spatial resolutions were changed.

The selection of environmental variables is the key to the operation of the mode, directly influencing both niche analysis results and the prediction of the eventual possible distribution area. The evaluation of the model results can be improved by removing the multiple collinearities of environmental variables. Numerous studies have reported that the multi-ollinearity between the selected environmental variables can cause the model to become overfit and impact the assessment of the model results (Sheppard, 2013; Feng et al., 2019; Wang et al., 2024). Therefore, to ensure the mutual independence of environmental variables, we conducted Pearson's correlation analysis on the 40 environmental variables included in this study. Subsequently, the 40 environmental variables were filtered by the MaxEnt model, eliminating factors with a contribution rate lower than 1.00%. In addition, variables with scores lower than 0.10 in the regularization training gain were removed, as low contributing environmental variables can lead

to a decrease in the accuracy of the model's predictions. Finally, if the Pearson's correlation coefficient between the two environmental variables has an absolute value exceeding 0.80 ($|r|>0.80$), only the variables exhibiting a higher contribution rate were selected following the approach proposed to reduce the occurrence of model overfitting (Cao et al., 2016). Finally, we selected 16 environmental variables with less Pearson's correlation ($|r|<0.80$) (Fig. 2; Table S2). As the environmental parameters of the final model, they were entered into the MaxEnt software for predicting the ranges and habitats of the six halophytic plant species.

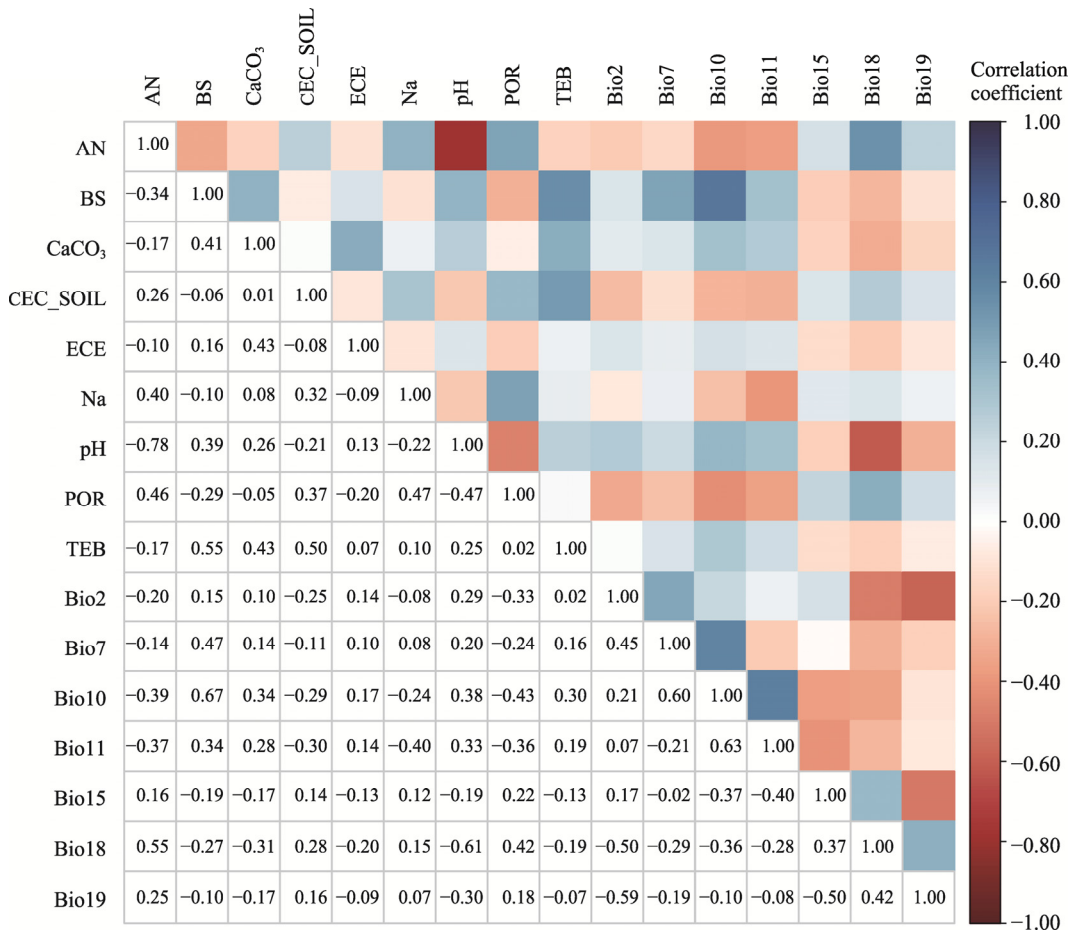

Fig. 2 Pearson's correlation analysis of the 16 selected environmental variables. AN, available nitrogen; BS, soil base saturation; $CaCO_3$, soil calcium carbonate; CEC_SOIL, cation exchange capacity; ECE, electrical conductivity; Na, exchangeable Na^+; pH, acidity and basicity; POR, porosity; TEB, soil exchangeable base; Bio2, mean diurnal range; Bio7, temperature annual range; Bio10, mean temperature of the warmest quarter; Bio11, mean temperature of the coldest quarter; Bio15, precipitation seasonality (coefficient of variation); Bio18, precipitation of the warmest quarter; Bio19, precipitation of the coldest quarter.

2.4 Model construction and evaluation

Plant habitat suitability was modeled using a selected MaxEnt model (MaxEnt version 3.4.1; https://biodiversityinformatics.amnh.org/open_source/maxent/) (Elith et al., 2006; Phillips et al., 2009). The model training process used 75.00% of the species distribution records, and the remaining portion was allocated for model testing. The resilience of the model was assessed using 20 replicates. This involved setting 5000 maximum iterations and utilizing 10,000 background samples to achieve the optimal solution. The averages of the results were measured, with other parameters setting at default values. The model's accuracy was evaluated using the area under the receiver operating characteristic curve (AUC) (Na et al., 2018). Previous study has validated that

AUC is a reliable measure for both calibrating and validating the model's accuracy (Elith et al., 2011). The AUC value ranges from 0.50 (indicating that the model's accuracy is equivalent to that of a random model) to 1.00 (representing an ideal state where the model's predictions perfectly align with the actual outcomes). An AUC value close to 1.00 indicates the superior prediction ability of the model (Phillips et al., 2006). The widely adopted standard is that the AUC value falls between 0.00 and 1.00, with 0.50–0.60, 0.60–0.70, 0.70–0.80, 0.80–0.90, and >0.90 indicating failed, poor, general, good, and excellent performance, respectively (Srivastava et al., 2019; Tu et al., 2021; Yin et al., 2023). Furthermore, appropriateness maps were created by computing the potential habitat suitability index (varying from 0.00 to 1.00) for the species distribution using the logistic output of the MaxEnt model. On this scale, the index value of 0.00 indicates a completely unsuitable habitat, and the higher the index value, the greater the suitability. In ArcGIS 10.8 software, the suitability index was divided into four categories using natural breaks: 0.00–0.20, 0.20–0.40, 0.40–0.60, and 0.60–1.00 for non-suitable, low suitable, medium suitable, and high suitable areas, respectively (Zhang et al., 2019; Ye et al., 2021). The assessment of the distribution model's environmental predictor contributions was conducted by analyzing percentage variable contributions and employing the Jackknife program (Xiong et al., 2020). This test was employed to ascertain the impact of every independent variable within the model. The suitable range of environmental variables for the potential distribution of six halophytic plant species was identified (Table S3). On this basis, the possible changes and distribution dynamics of a suitable habitat area for plant species in the future were calculated. The predicted results of plant species for different periods were converted into binary distribution files. Further, the change trend of suitable areas was computed through the SDM toolbox, and the shrinking, expanding, and stable regions for plant species distribution were obtained. The Centroid Shift toolbox in the SDM toolbox was used to obtain the centroids of the suitable habitat areas. The migration routes of high suitable habitats can be obtained by observing the movement of centroids in high suitable habitats (Cong et al., 2020) and comparing the future centroid with the existing centroid (Brown, 2014).

3 Results

3.1 Evaluation of the simulation results

The MaxEnt model was employed to forecast the possible spread of six halophytic plant species in various timeframes, both in the current and in the future. The average AUC value was >0.80 (Table 1); therefore, the model's predictions were considered to be of good quality. This study accurately and reliably simulated the suitable ranges of six halophytic plant species under various climate scenarios, employing the MaxEnt model.

Table 1 Area under the receiver operating characteristic curve (AUC) values of six halophytic plant species under the current climate conditions and future climate scenarios based on the maximum entropy (MaxEnt) model

Species	AUC						
	1970–2000	SSP245			SSP585		
		2050s	2070s	2090s	2050s	2070s	2090s
S. salsa	0.85±0.05	0.85±0.03	0.85±0.05	0.84±0.07	0.83±0.04	0.84±0.04	0.83±0.04
S. europaea	0.83±0.05	0.83±0.05	0.82±0.04	0.82±0.03	0.80±0.05	0.83±0.06	0.83±0.04
H. glomeratus	0.89±0.02	0.89±0.02	0.89±0.03	0.89±0.03	0.88±0.02	0.89±0.03	0.89±0.03
H. strobilaceum	0.91±0.02	0.92±0.03	0.94±0.03	0.92±0.03	0.93±0.03	0.93±0.02	0.93±0.03
K. foliatum	0.83±0.01	0.85±0.03	0.83±0.03	0.83±0.03	0.83±0.02	0.84±0.02	0.82±0.02
H. caspica	0.84±0.02	0.86±0.02	0.86±0.02	0.85±0.02	0.86±0.01	0.86±0.02	0.85±0.02

Note: *S. salsa*, *Suaeda salsa* (L.) Pall.; *S. europaea*, *Salicornia europaea* L.; *H. glomeratus*, *Halogeton glomeratus* (Bieb.) C. A. Mey.; *H. strobilaceum*, *Halocnemum strobilaceum* (Pall.) Bieb.; *K. foliatum*, *Kalidium foliatum* (Pall.) Moq.; *H. caspica*, *Halostachys caspica* (Bieb.) C. A. Mey. SSP, Shared Socio-economic Pathway. Mean±SD.

3.2 Contribution rates of environmental variables

The average contribution rates and suitability ranges of environmental variables (Tables S2 and S3) indicated that precipitation seasonality (coefficient of variation) (Bio15), precipitation of the warmest quarter (Bio18), and soil factor exchangeable Na^+ (Na) exhibited the highest contribution rates (23.15%, 13.22%, and 11.68%, respectively). Among the temperature variables, the average contribution of the mean temperature of the warmest quarter (Bio10) contributed at the highest level, reaching 4.90%. There were significant differences in the contribution of the same environmental variable to each plant species. For example, the contribution rates of Bio15 for *H. glomeratus*, *H. strobilaceum*, and *H. caspica* were 44.00%, 32.00%, and 23.40%, respectively. The suitable ranges of Bio15 for these three species were 23.26–70.13, 23.26–68.34, and 23.22–76.41 mm, respectively. However, the contribution rates of Bio15 for *S. salsa* and *K. foliatum* were only 1.70% and 2.00%, respectively. The suitable ranges of Bio15 for *S. salsa* and *K. foliatum* were 82.27–111.27 and 37.17–80.05 mm, respectively. Additionally, Bio10 was a secondary factor affecting the distribution of *K. foliatum*, with a suitable range from –10.33°C to –1.82°C. In addition, among the soil factors, Na was the key factor for *S. salsa*, *S. europaea*, *H. caspica*, and *K. foliatum*, and the suitable range was from 0.11 to 0.17 cmol/kg.

The Jackknife test results indicated that when the variables were used alone, Bio15 exhibited the greatest gain for *H. strobilaceum*, *H. glomeratus*, and *H. caspica*, and Bio18 exhibited the greatest gain for *K. foliatum* (Fig. 3). These variables were considered to have the most information about the species distribution. The soil factor Na exhibited a higher gain than other variables for *S. salsa* and *S. europaea*.

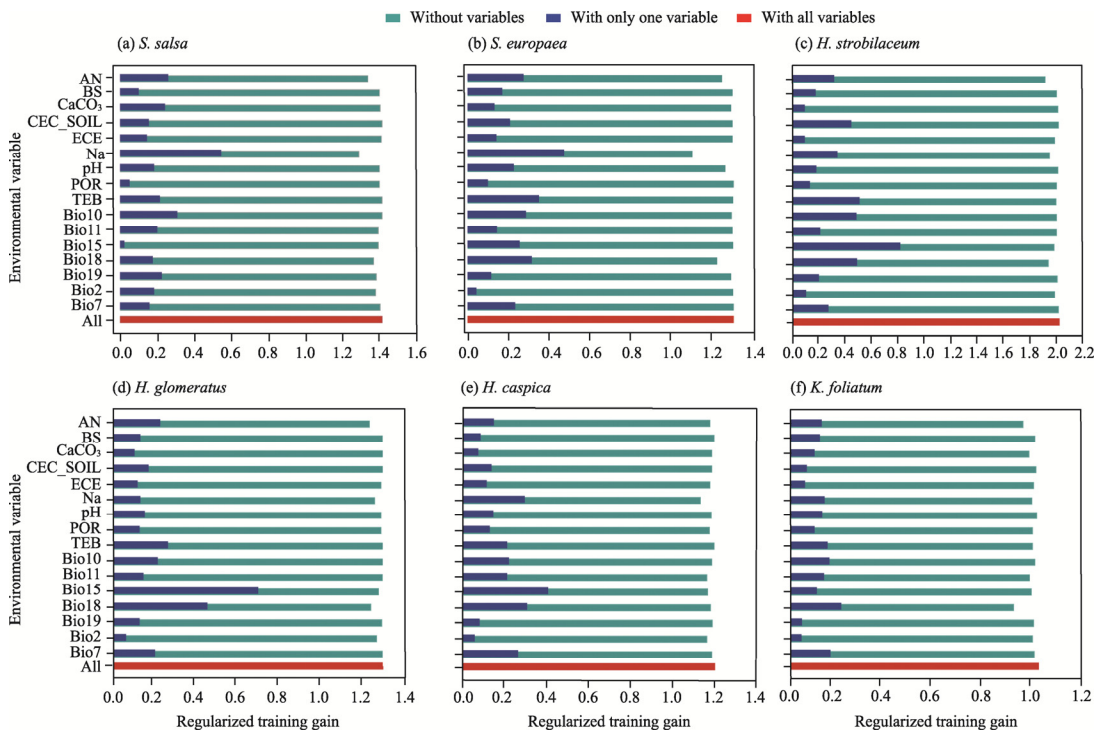

Fig. 3 Contribution rates of the selected 16 environmental variables to the distribution of six halophytic plant species based on the Jackknife test. (a), *S. salsa*; (b), *S. europaea*; (c), *H. strobilaceum*; (d), *H. glomeratus*; (e), *H. capsica*; (f), *K. foliatum*.

3.3 Current potential distribution of six halophytic plant species

According to the prediction of the MaxEnt model, different plant species exhibited different characteristics in terms of the area and location of suitable habitats (Fig. 4). The total suitable habitat area (the sum of low, medium, and high suitable areas) for *S. salsa* was 92.60×10^4 km^2;

the medium and high suitable habitats were primarily distributed in central Ningxia, southern Xinjiang, Shaanxi, Inner Mongolia, and parts of Gansu (Fig. 4a). The total suitable habitat areas for *S. europaea* and *H. caspica* were 112.00×10^4 and 118.00×10^4 km^2, respectively, predominantly located in Xinjiang, Inner Mongolia, and northern Ningxia (Fig. 4b and e, respectively). The minimum distribution of the suitable habitat area for *H. strobilaceum* was approximately 47.40×10^4 km^2, and the medium and high suitable habitats were predominantly located in Xinjiang and sporadically distributed in Gansu and Inner Mongolia (Fig. 4c). The total suitable habitat area for *H. glomeratus* was 99.10×10^4 km^2; the medium and high suitable habitats were predominantly situated in Xinjiang and sporadically distributed in Inner Mongolia (Fig. 4d). The maximum total area of suitable habitat for *K. foliatum* was approximately 150.00×10^4 km^2, mainly in Xinjiang, northern Ningxia, central Gansu, central Qinghai, and southwestern Inner Mongolia (Fig. 4f).

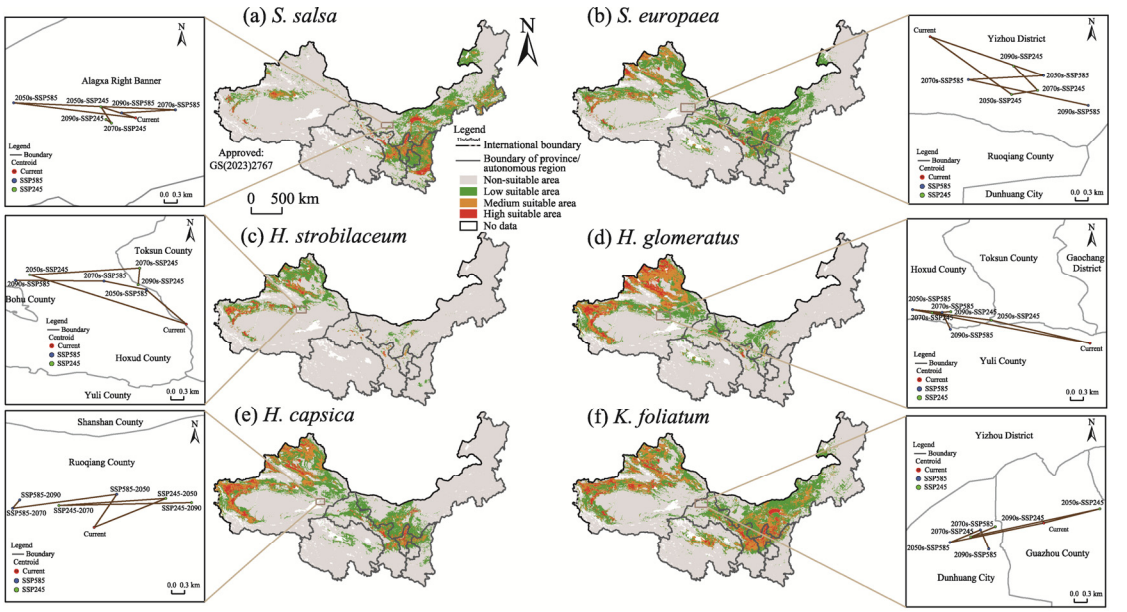

Fig. 4 Predicted current distribution ranges and changes in the centroid distribution of six halophytic plant species in the future (2050s, 2070s, and 2090s) under two climate scenarios (SSP245 and SSP585) in the arid areas of Northwest China. (a), *S. salsa*; (b), *S. europaea*; (c), *H. strobilaceum*; (d), *H. glomeratus*; (e), *H. capsica*; (f), *K. foliatum*. SSP, Shared Socio-economic Pathway. Note that the figures are based on the standard map (GS(2023)2767) of the Map Service System (http://bzdt.ch.mnr.gov.cn/) marked by the Ministry of Natural Resources of the People's Republic of China, and the boundary of the standard map has not been modified.

3.4 Future changes in the suitable habitat areas of six halophytic plant species

Based on the circumstances of SSP245 and SSP585, the suitable habitat areas for different halophytic plant species in the future (2050s, 2070s, and 2090s) will experience different contraction and expansion movements relative to the current situation (Table 2; Fig. 5). Overall, compared with the suitable distribution range in the current situation, the suitable habitat area of *S. salsa* would only shrink by 0.85% under the SSP245 scenario in the 2050s; later, it would continue to expand with a maximum expansion area of approximately 16.11% under the SSP585 scenario in the 2050s (Fig. 6). Under the SSP245 and SSP585 scenarios, the suitable habitat area of *S. europaea* would be reduced by 9.00% and 9.18% in the 2050s, respectively (Fig. 7). The suitable habitat area for *H. glomeratus* would shrink completely under the two future climate scenarios (Fig. 8). Specifically, under the SSP585 scenario, the maximum contraction of the suitable habitat for *H. glomeratus* in the 2050s would be nearly 15.30%. The suitable habitat area of *H. strobilaceum* would be reduced by 10.72% in the 2050s and 4.01% in the 2090s (Fig. 9). On the other hand, the suitable habitat area of *H. caspica* would shrink by 1.29% and 3.82% in the 2070s and 2090s under the SSP245 scenario, respectively, and reduce by 4.66% in the 2070s

under the SSP585 scenario (Fig. 10). Under the future climate scenarios, complete expansion would be observed in the suitable habitat area of *K. foliatum*, with the maximum expansion of the suitable habitat being nearly 6.27% in the 2050s (Fig. 11).

Table 2 Change rates of the suitable habitat area for the six halophytic plant species in the future (2050s, 2070s, and 2090s) under two climate scenarios (SSP245 and SSP585) compared to the current conditions

Species	Change rate of the suitable habitat area (%)					
	SSP245			SSP585		
	2050s	2070s	2090s	2050s	2070s	2090s
S. salsa	–0.85	8.63	11.95	16.11	6.73	6.90
S. europaea	–9.00	0.54	0.43	–9.18	–2.21	1.79
H. strobilaceum	–10.72	4.16	–4.01	6.20	5.57	6.67
H. glomeratus	–12.53	–10.56	–13.95	–12.89	–15.30	–4.61
H. caspica	2.56	–1.29	–3.82	2.87	–4.66	2.94
K. foliatum	3.35	1.40	5.95	3.60	6.27	2.14

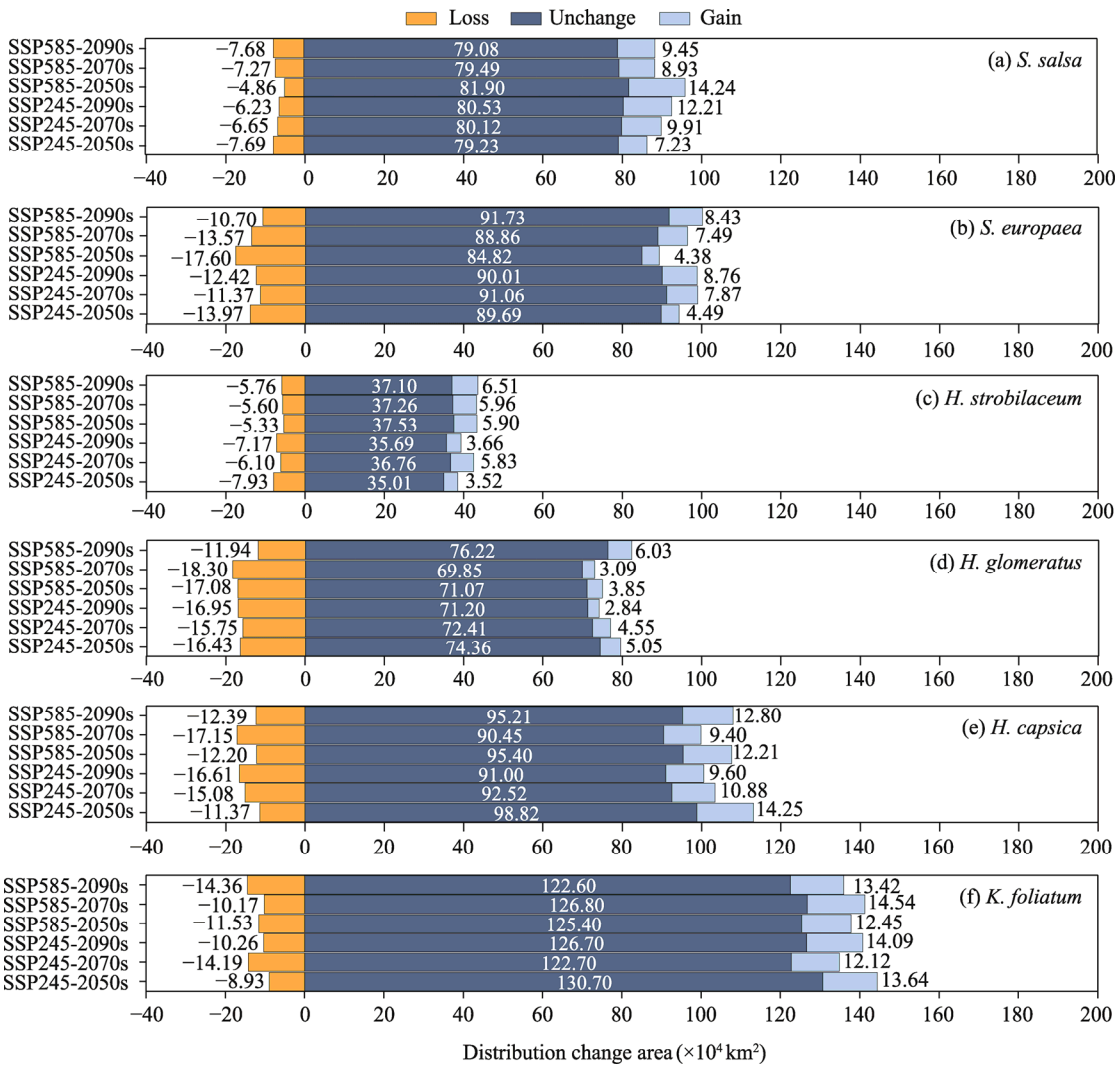

Fig. 5 Distribution change areas of the suitable habitats for the six halophytic plant species in the future (2050s, 2070s, and 2090s) under two climate scenarios (SSP245 and SSP585) compared to the current conditions. (a), *S. salsa*; (b), *S. europaea*; (c), *H. strobilaceum*; (d), *H. glomeratus*; (e), *H. capsica*; (f), *K. foliatum*.

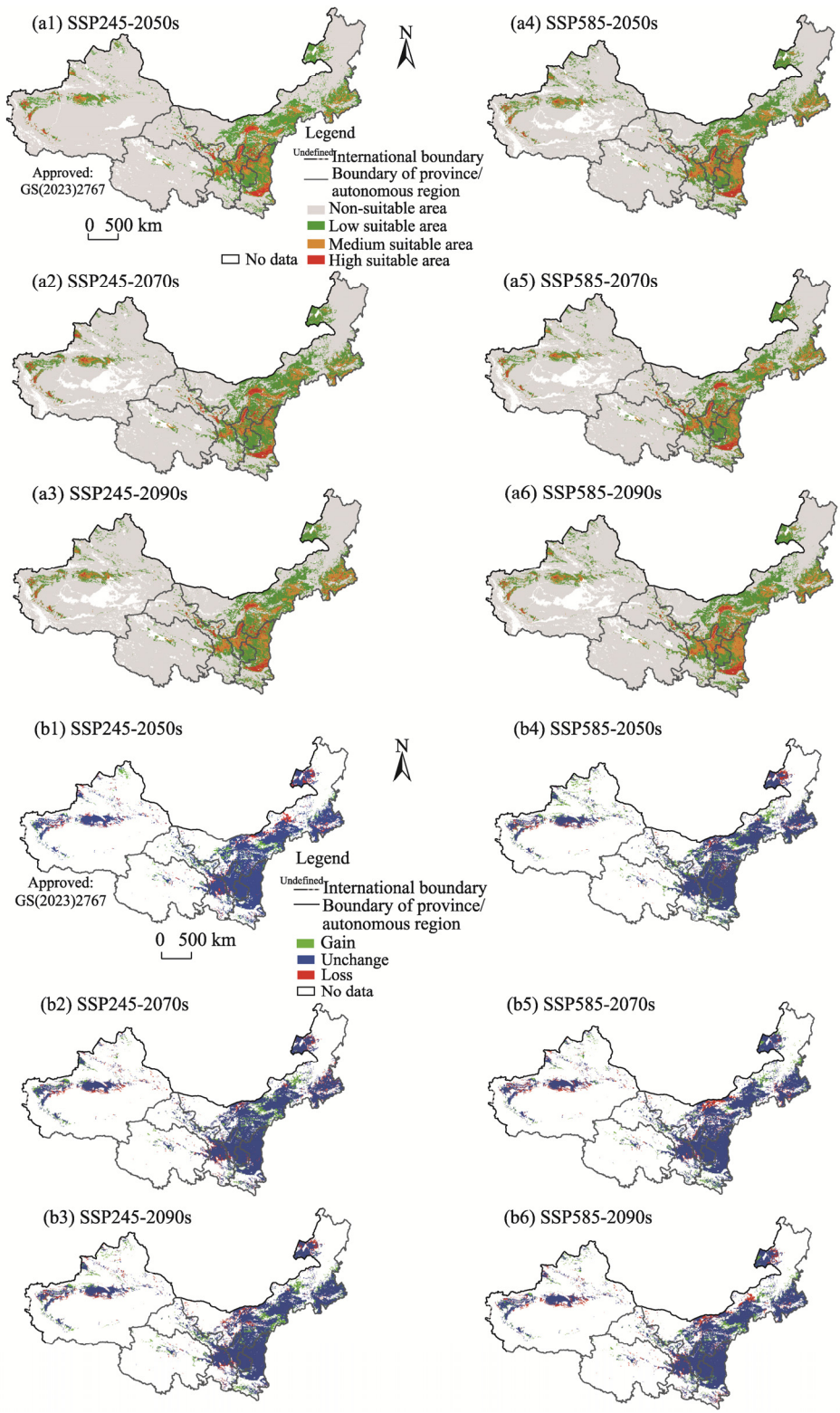

Fig. 6 Potential suitable habitats (a1, a2, a3, a4, a5, and a6) and changes in the distribution ranges (b1, b2, b3, b4, b5, and b6) of *S. salsa* in the future (2050s, 2070s, and 2090s) under two climate scenarios (SSP245 and SSP585) compared to its current distribution in the arid areas of Northwest China. Note that the figures are based on the standard map (GS(2023)2767) of the Map Service System (http://bzdt.ch.mnr.gov.cn/) marked by the Ministry of Natural Resources of the People's Republic of China, and the boundary of the standard map has not been modified.

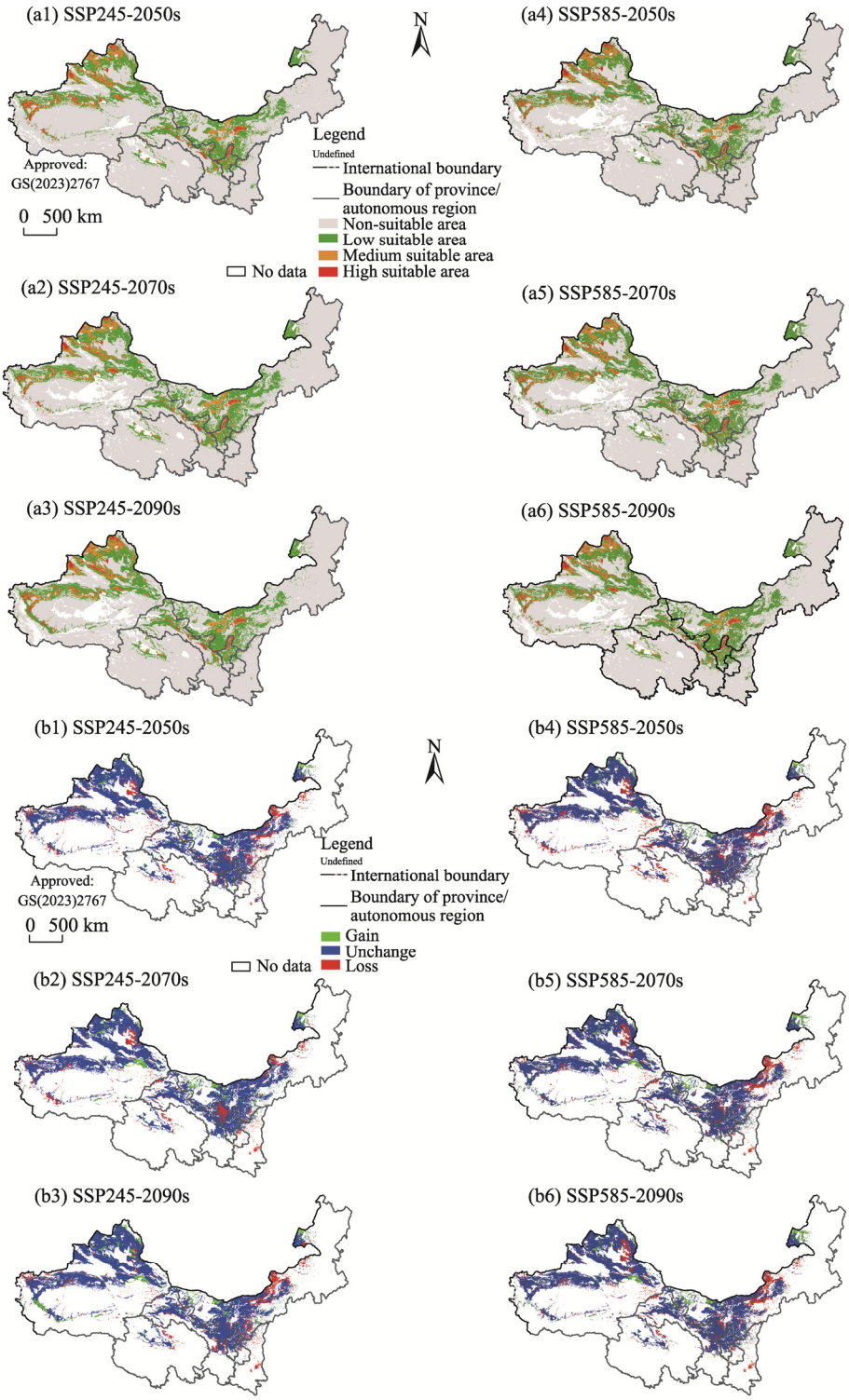

Fig. 7 Potential suitable habitats (a1, a2, a3, a4, a5, and a6) and changes in the distribution range (b1, b2, b3, b4, b5, and b6) of *S. europaea* in the future (2050s, 2070s, and 2090s) under two climate scenarios (SSP245 and SSP585) compared to its current distribution in the arid areas of Northwest China. Note that the figures are based on the standard map (GS(2023)2767) of the Map Service System (http://bzdt.ch.mnr.gov.cn/) marked by the Ministry of Natural Resources of the People's Republic of China, and the boundary of the standard map has not been modified.

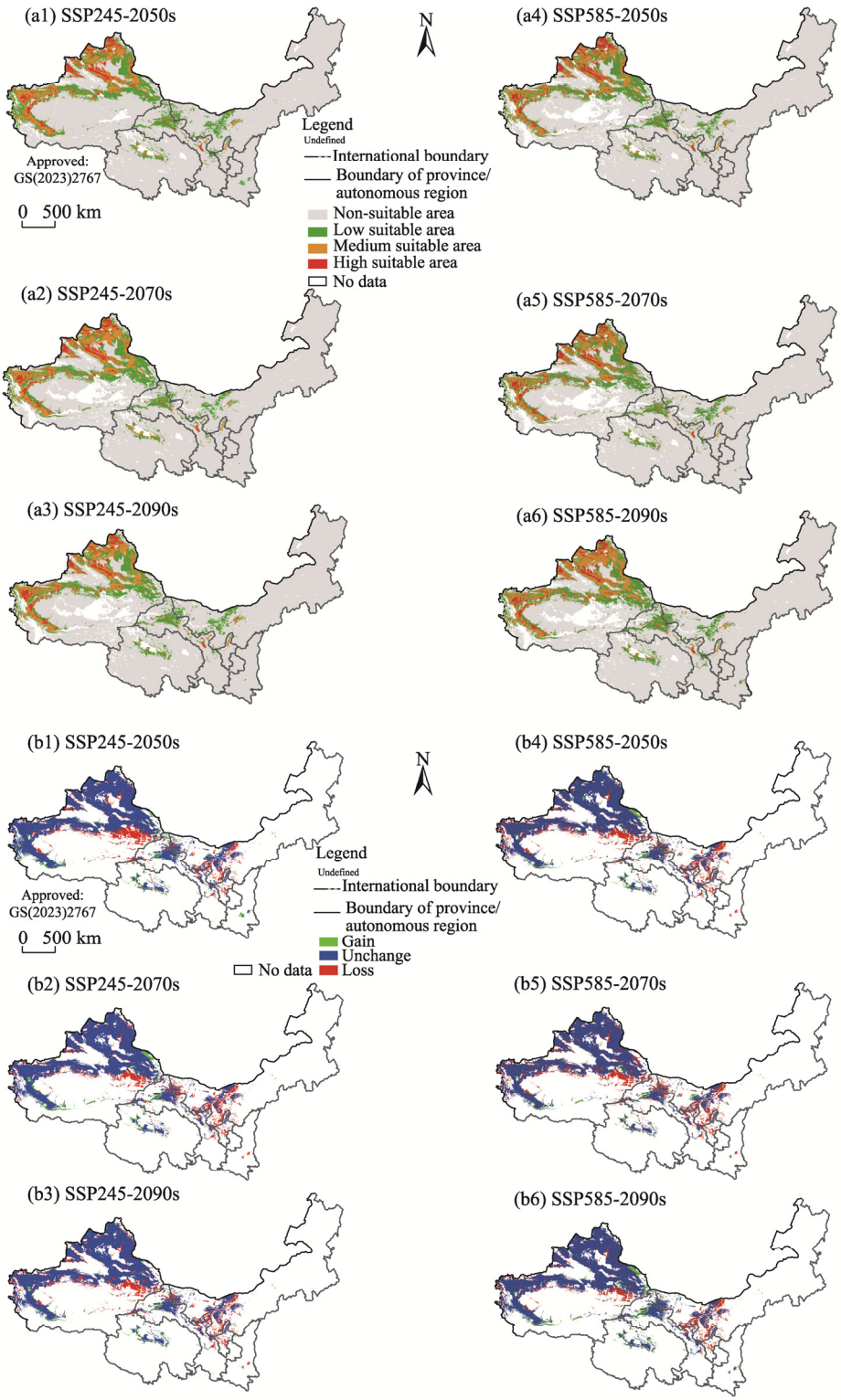

Fig. 8 Potential suitable habitats (a1, a2, a3, a4, a5, and a6) and changes in the distribution range (b1, b2, b3, b4, b5, and b6) of *H. glomeratus* in the future (2050s, 2070s, and 2090s) under two climate scenarios (SSP245 and SSP585) compared to its current distribution in the arid areas of Northwest China. Note that the figures are based on the standard map (GS(2023)2767) of the Map Service System (http://bzdt.ch.mnr.gov.cn/) marked by the Ministry of Natural Resources of the People's Republic of China, and the boundary of the standard map has not been modified.

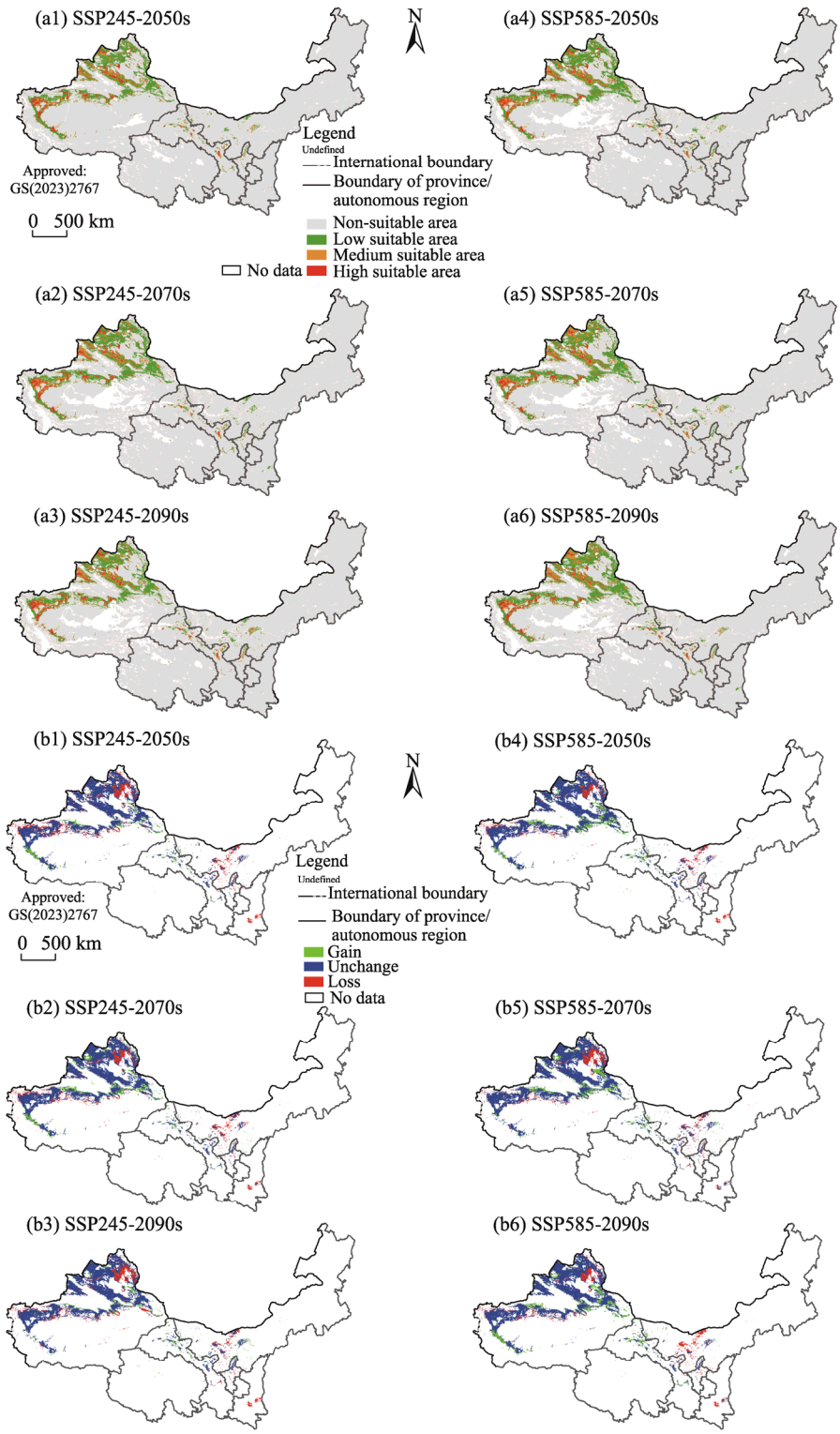

Fig. 9 Potential suitable habitats (a1, a2, a3, a4, a5, and a6) and changes in the distribution range (b1, b2, b3, b4, b5, and b6) of *H. strobilaceum* in the future (2050s, 2070s, and 2090s) under two climate scenarios (SSP245 and SSP585) compared to its current distribution in the arid areas of Northwest China. Note that the figures are based on the standard map (GS(2023)2767) of the Map Service System (http://bzdt.ch.mnr.gov.cn/) marked by the Ministry of Natural Resources of the People's Republic of China, and the boundary of the standard map has not been modified.

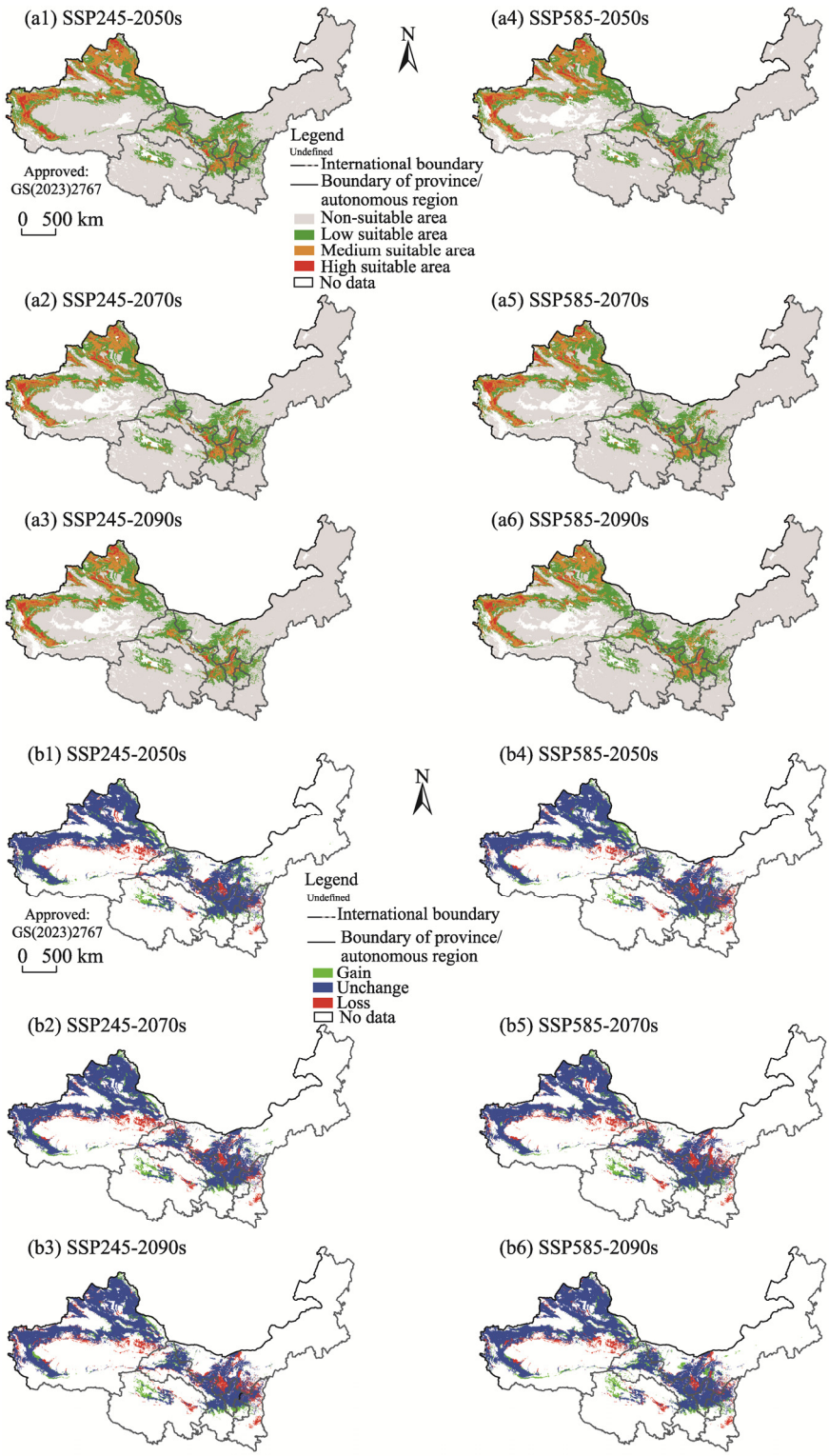

Fig. 10 Potential suitable habitats (a1, a2, a3, a4, a5, and a6) and changes in the distribution range (b1, b2, b3, b4, b5, and b6) of *H. caspica* in the future (2050s, 2070s, and 2090s) under two climate scenarios (SSP245 and SSP585) compared to its current distribution in the arid areas of Northwest China. Note that the figures are based on the standard map (GS(2023)2767) of the Map Service System (http://bzdt.ch.mnr.gov.cn/) marked by the Ministry of Natural Resources of the People's Republic of China, and the boundary of the standard map has not been modified.

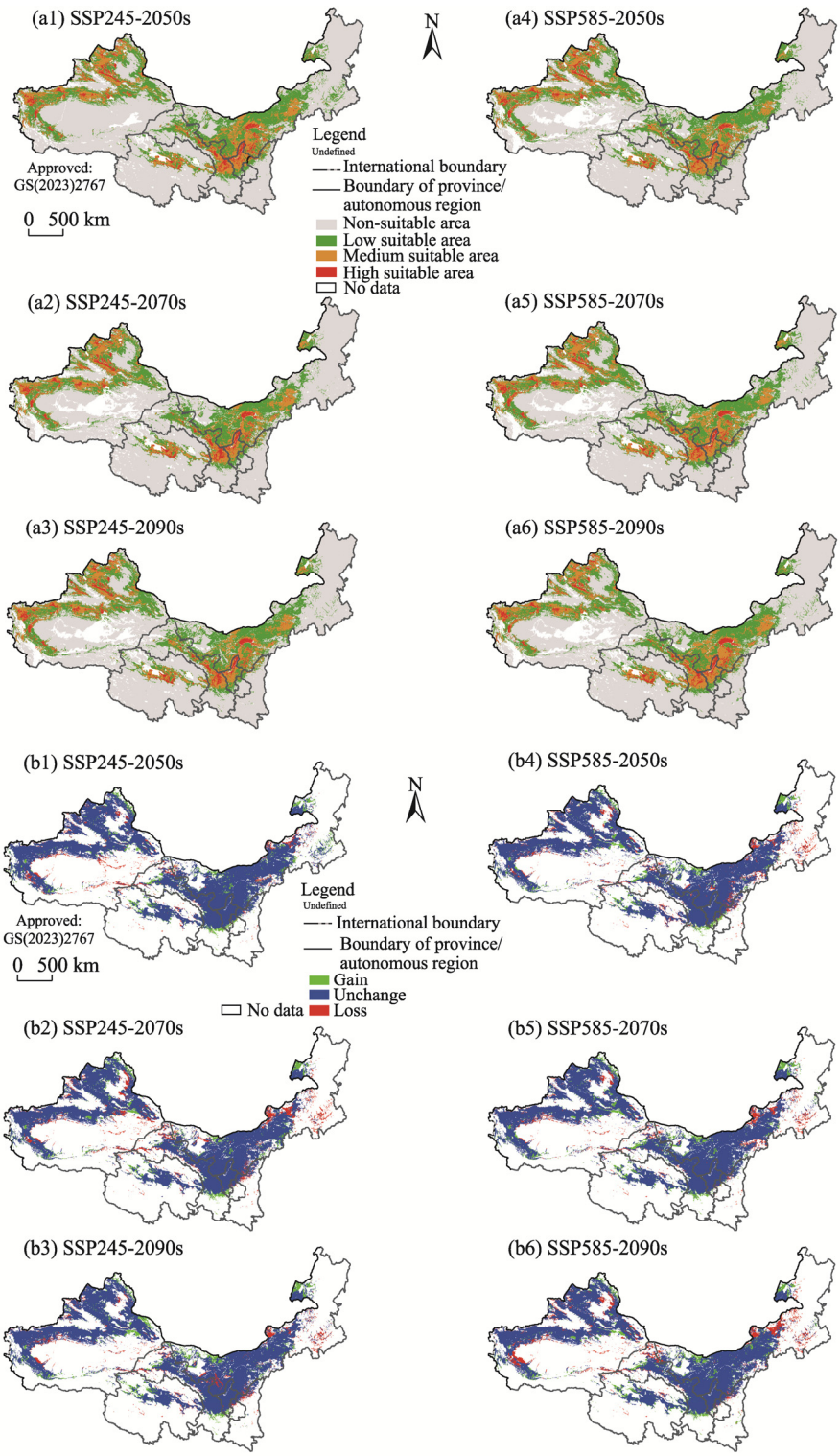

Fig. 11 Potential suitable habitats (a1, a2, a3, a4, a5, and a6) and changes in the distribution range (b1, b2, b3, b4, b5, and b6) of *K. foliatum* in the future (2050s, 2070s, and 2090s) under two climate scenarios (SSP245 and SSP585) compared to its current distribution in the arid areas of Northwest China. Note that the figures are based on the standard map (GS(2023)2767) of the Map Service System (http://bzdt.ch.mnr.gov.cn/) marked by the Ministry of Natural Resources of the People's Republic of China, and the boundary of the standard map has not been modified.

In the future (2050s, 2070s, and 2090s), the distribution areas of the suitable habitats for the six halophytic plant species under the SSP245 and SSP585 scenarios would gain or lose to varying degrees compared with the current conditions (Figs. 6–11). For *S. salsa*, the gain in the suitable habitat area would be 7.23×10^4–14.24×10^4 km^2 in eastern Inner Mongolia, Xinjiang, and Gansu, and the loss in the suitable habitat area would be 4.86×10^4–7.69×10^4 km^2, mainly in Inner Mongolia. It is predicted that for *S. europaea*, the gain in the suitable habitat area would be 4.38×10^4–8.76×10^4 km^2 in the eastern part of western and easternmost regions of Inner Mongolia and the Turpan Basin of Xinjiang, whereas the loss in the suitable habitat area would be 3.15×10^4–6.96×10^4 km^2, mainly in northern Xinjiang, central-eastern part of Inner Mongolia, and Qinghai. For *H. strobilaceum*, the suitable habitat area would greatly increase in Xinjiang and sporadically increase in Gansu and Inner Mongolia, with the gain of 3.52×10^4–6.51×10^4 km^2, whereas the loss in the suitable habitat area would be 5.33×10^4–7.93×10^4 km^2 in northern Xinjiang and central-eastern part of Inner Mongolia. For *H. glomeratus*, the suitable habitat area would sporadically increase in southern Xinjiang and Qinghai, with the gain of 2.84×10^4–6.03×10^4 km^2, whereas the loss in the suitable habitat area would be 11.94×10^4–18.30×10^4 km^2 in eastern Xinjiang and central Inner Mongolia. For *H. caspica*, the gain in the suitable habitat area at high latitudes would be 9.40×10^4–14.25×10^4 km^2, whereas the loss in the suitable habitat area would be 11.37×10^4–17.15×10^4 km^2 at low latitudes. The suitable habitat range of *K. foliatum* would gain eastward and northward along the distribution boundary of the current habitats, with the gain area of 12.12×10^4–14.54×10^4 km^2 and the loss area of 8.93×10^4–14.36×10^4 km^2.

3.5 Changes in the centroids of the suitable habitats of six halophytic plant species

At present, the centroid of the suitable habitat for *S. salsa* is located in the Alagxa Right Banner of Inner Mongolia (Fig. 4a). In the future, the centroid of the suitable habitat for *S. salsa* would be projected to shift to high latitudes under the SSP585 scenario. At present, the centroid of the suitable habitat for *S. europaea* is located in the southeast of Yizhou District, Hami City, Xinjiang (Fig. 4b). In the future, it would generally shift to the eastern region. At present, the centroid of the suitable habitat for *H. strobilaceum* is located in the western part of Toksun County, Xinjiang (Fig. 4c), and it would be generally shifted to the western part and high latitudes in the future. At present, the centroid of the suitable habitat for *H. glomeratus* is located in the northeast of Yuli County, Xinjiang (Fig. 4d), and it would shift to the east and high latitudes in the future under the two climate scenarios. At present, the centroid of the suitable habitat for *H. caspica* is located in the northern part of Ruoqiang County, Xinjiang (Fig. 4e), and in the future, this centroid will generally shift to high latitudes in the northern region relative to its present location. The centroid of the suitable habitat for *K. foliatum* is currently located in the central part of Guazhou County at the western end of Gansu (Fig. 4f). In the future, it would shift and alternately migrate along the east–west direction and generally be in Dunhuang City, Gansu under the SSP245 scenario.

4 Discussion

4.1 Reliability of the MaxEnt model

In this study, the suitable habitats of *S. salsa*, *S. europaea*, *H. glomeratus*, *H. strobilaceum*, *K. foliatum*, and *H. caspica* in the arid areas of Northwest China were predicted in the future under two climate scenarios. The predicted AUC values for all plant species using the MaxEnt model were higher than 0.80, which met the evaluation criteria and had high accuracy (Phillips et al., 2006). In our study, the geographical occurrence data of the halophytic plant species were processed using the data processing strategy proposed by previous studies to prevent the overfitting of the model (Phillips and Dudík, 2008; Kramer-Schadt et al., 2013; Merow et al., 2013; Warren et al., 2014). The ENMTools software was used to optimize the species occurrence records and reduce the possibility of overfitting the model due to data problems. The MaxEnt model has demonstrated great accuracy and superiority over alternative approaches, even when

available species occurrence data are scarce (Hernandez et al., 2006; Gogol-Prokurat, 2011). For instance, Gogol-Prokurat (2011) employed the MaxEnt model for predicting the species distribution to forecast the habitat suitability of uncommon plant species on a small geographical scale in El Dorado County, California, USA. Zhang and Zhao (2021) employed the MaxEnt model to predict biodiversity hotspots for rare and endangered plant species in Northwest China, providing scientific insights for habitat restoration and reconstruction efforts. Huang et al. (2019) used the MaxEnt model to predict the suitable habitat ranges of five plant species belonging to the genus of *Zingiber* in China; their results indicated that under climate change, the suitable habitats for most *Zingiber* species will significantly decrease, highlighting the need for the conservation of these plant resources. Therefore, the MaxEnt model is suitable for analyzing the current and future habitat distributions of the studied six halophytic plant species, namely, *S. salsa*, *S. europaea*, *H. glomeratus*, *H. strobilaceum*, *K. foliatum*, and *H. caspica*, in saline environments.

4.2 Important influence of environmental variables on the distribution of halophytic plant species

Pearson's correlation analysis and Jackknife test method were used to identify the primary environmental variables that impact the distribution of halophytic plant species (Elith et al., 2011; Fourcade et al., 2018). Finally, 16 environmental variables were selected for use in the MaxEnt model, and the contribution rates (Table S2) and suitable habitat ranges (Table S3) were obtained. The results revealed that climate was the primary environmental factor influencing the distribution of halophytic plant species compared with soil factors (Li et al., 2022). The contribution of three precipitation variables (Bio15, Bio18, and precipitation of the coldest quarter (Bio19)) to the distribution of six halophytic plant species was 40.98%. Previous studies have highlighted the significant influence of precipitation on the distribution patterns of plant species (Abolmaali et al., 2017; Khajoei Nasab et al., 2020; Liu et al., 2021). Precipitation affects the distribution patterns of plant species through its impact on seed germination, seedling development and survival, and phenology (Quevedo-Robledo et al., 2010; Mathias and Chesson, 2013). Future climate scenarios, including changes in precipitation, will influence the variations in different plant species in terms of positive or negative responses. For halophytes growing in saline–alkaline land in arid and semi-arid areas, if precipitation decreases in the future, the distribution pattern and suitable habitat area of plant species will significantly change (Song et al., 2023). For example, the distribution pattern of plant species will shift to higher latitudes and suitable habitat area will face loss and fragmentation, as the decrease of precipitation.

The contribution of temperature variables to the distribution of six halophytic plant species was 14.88% (Table S2). Of them, the contribution of Bio10 to the distribution of *K. foliatum*, *H. strobilaceum*, and *S. salsa* was relatively high among the temperature variables. Qu et al. (2008) reported that the germination rate of *H. strobilaceum* was higher at high temperatures than at low temperatures. Wang et al. (2019) discovered that the best germination temperature for *S. glauca* ranges from 10.00°C to 20.00°C. Different plant species exhibit different reponses to temperature; therefore, global warming may increase the distribution range of *S. salsa*, *K. foliatum*, and other halophytic plant species. According to recent research, temperature may significantly affect the potential distribution of halophytic plant species (Ardestani et al., 2015; Ma and Sun, 2018; Zhao et al., 2021). Precipitation significantly influences plant diversity in arid and semi-arid areas (Gessner et al., 2013; Li et al., 2013), followed by heat conditions in the growing season. Therefore, changes in precipitation and temperature exert a notable influence on the distribution of halophytic plant species, affecting plant development and seedling survival (Poorter, 2000).

In addition to climate variables, soil is another key environmental factor that influences the changes of suitable habitat and distribution of halophytic plant species. Alterations in the soil's physical and chemical characteristics, in addition to changes in the composition of bedrock, can affect the distribution of halophytic plant species (Piedallu et al., 2011). The tendency for soil salinization can be accelerated by increases in temperature and sea level, decrease in precipitation, and ineffective irrigation management (Eswar et al., 2021). *S. salsa*, *K. foliatum*, *H.*

capsica, and *S. europaea* were greatly affected by soil factors, including Na. Excessive salt content in the soil reduces plant water absorption, disrupts metabolism, and inhibits plant growth (van Zelm et al., 2020). *S. salsa* exhibits moderate tolerance to salt stress (Wang et al., 2019); however, *K. foliatum* and *H. caspica* show strong tolerance to salt stress. The combination of drought and salinity can hinder plant growth (Lu et al., 2021a). In this study, the contribution rate of available nitrogen (AN) to *H. glomeratus* was the highest with the suitable range of 41.11–109.77 mg/kg, and that of cation exchange capacity (CEC_SOIL) to *H. strobilaceum* was the highest with the suitable range of 1.00–1.69 cmol/kg. This is consistent with the study by Nilhan et al. (2008) on the impact of CEC_SOIL on the distribution of *H. strobilaceum*. The content of soil organic matter significantly influences the occurrence and distribution of halophytic plant species. Recent research has indicated that soil variables significantly influence the distribution of halophytic plant species (Yilmaz et al., 2017; Khajoei Nasab et al., 2020).

4.3 Changes in the suitable habitats of halophytic plant species

Changes in precipitation, temperature, and other components of human-induced climate change alter the species distribution on a global or local level (Pecl et al., 2017). Species distribution ranges would expand, contract, or remain unchanged due to global warming (Petitpierre et al., 2016). In this study, various halophytic plant species exhibited distinct ecological habits in response to climate change. As the impact of climate change worsen in the future, the suitable distribution range of *S. salsa* will expand with global warming and there is a trend of westward and nearby expansion (Fig. 6). This may be related to the fact that the developmental state of *S. salsa* is directly impacted by water and salt (An et al., 2019). The suitable habitat area of *S. europaea* would significantly decrease in the 2050s under two climate scenarios. However, the habitat loss area would gradually decrease and become fragmented, which is obvious in northern Xinjiang, Inner Mongolia, and Qinghai (Fig. 7). *S. europaea* was observed to be relatively highly affected by precipitation and soil variables (including Na and pH). Climate change impacts plant water supplies and hinders seed germination (Shi et al., 2021). The suitable habitat area of *H. glomeratus* would shrink to varying degrees at any time and under any climate scenario in the future, and the shrinking trends would occur in Inner Mongolia and Xinjiang (Fig. 8). The shrinkage of the suitable habitat area for *H. glomeratus* in the future may be affected by the gradual decrease in precipitation and increase in temperature (Korell et al., 2021). One of the primary influential factors in habitat fragmentation is thought to be climate change (Yi et al., 2016; Qin et al., 2017). For example, the suitable habitat range of the globally cultivated *Xanthium italicum* Moretti will shrink in the future due to climate change (Zhang et al., 2021). Although the current study is not directly related to habitat fragmentation, shifts in species distribution by climate change are very likely to result in habitat fragmentation. Habitat fragmentation can lead to a reduction in local plant species populations and the flow of genes from other populations (Wu et al., 2014). As a result, adaptability, genetic variation, and diplomacy will be reduced (Wang et al., 1998). The suitable habitat area of *H. strobilaceum* will exhibit complete expansion under the SSP585 scenario in the future (Fig. 9); currently, this species also faces the risk of habitat loss in northern Xinjiang and Inner Mongolia. This is consistent with the results of Bezeng et al. (2017) regarding the expected effects of climate change on 162 non-indigenous plant species in South Africa. Bezeng et al. (2017) indicated the likely expansion of species ranges in specific areas by the 2070s. The change in the distribution area of *H. caspica* would exhibit some fluctuations. Contraction and expansion of suitable habitat area are equally possible, but the scope of change is minimal. An obvious contraction would occur in the central and eastern Xinjiang and in the intersecting area of Ningxia and eastern Inner Mongolia (Fig. 10). Climate change can lead to insufficient water and excessive salt content in the soil (Hassani et al., 2021). Although the suitable habitat area of *K. foliatum* shows a trend toward complete expansion in the future, this species will face the risk of habitat loss in the eastern part of Inner Mongolia and in the Taklimakan Desert of Xinjiang due to changes of precipitation variables (Fig. 11). Increased soil salt content leads to decreased seed germination rate, and

temperature, precipitation, soil salinity, and their interactions further affect seed germination (Zhang et al., 2012). Climate change may be good or bad for the living conditions of some halophytic plant species (Lososová et al., 2018). For example, the distribution of six endangered saproxylics was predicted by integrating diffusion, land use change, and climate change (Rocca and Milanesi, 2020); the findings indicated that the distributions of four of the six halophytic plant species in our study were positively impacted by climate change.

It is very important to protect the shrinking habitat area of halophytes in the arid areas of Northwest China, which will be further exacerbated by global warming and the ensuing drought in the future (Qiu et al., 2017). To adapt to climate change, many halophytes would shift to more favorable habitats or face extinction; therefore, climate has an important impact on the distribution patterns of halophytic plant species (Corlett and Westcott, 2013). The spatiotemporal dynamics of widely distributed plant species should be detected and studied in detail (Collen et al., 2016). The impact of habitat fragmentation on the adaptation of halophytes to future climate change should also be further studied in detail.

Climate change impacts the migration of the suitable habitats of halophytic plant species (Richman et al., 2020). In the 2050s, the future centroid of the suitable habitat for *K. foliatum* would shift to the southwest after eastward migration under the SSP245 scenario, mainly due to the influences of temperature and precipitation (Corlett and Westcott, 2013). Although the centroids of the suitable habitats of *S. salsa*, *H. capsica*, *H. glomeratus*, and *H. strobilaceum* would shift to high latitudes with global warming, the migration distance among plant species would be different; the maximum shift distance of the centroid for each plant species would be 43.35–132.89 km, with variances for widely and narrowly distributed species. Plant species with restricted distributions are more susceptible to climate change because of their limited ecological adaptability (Zhang et al., 2015; Ma and Sun, 2018). For example, *S. salsa* and *H. capsica* are more widely distributed, and their centroid migration is smaller. Plant species that are more adaptable to climate change will have wider distribution ranges (Hu et al., 2015).

Climate is a crucial ecological component. Plant species adapt to climate change by altering their geographical distribution, such as by moving to higher latitudes or altitudes to find favorable environmental conditions (Chen et al., 2011; Lehikoinen and Virkkala, 2016; Qin et al., 2017). The centroid displacement of the suitable habitats for the six halophytic plant species in the future under the SSP245 and SSP585 scenarios indicated a relatively weak migration in case of the moderate SSP245 scenario, which is the same for several plant species spread over the western and central regions of China in the future (Chen et al., 2019; Sun et al., 2020). Under climate change, halophytic plant species will migrate to more suitable climatic zones, adjust their phenological or physiological adaptations to the new climate conditions, or become extinct in response to climate change (Vitt et al., 2010). According to previous study, certain plant species have apparently started to migrate, and most of these species cannot keep up with the impact of climate change (Corlett and Westcott, 2013). For example, migration of halophytic plant species for suitable habitats is strongly correlated with precipitation, temperature, soil, and other factors. It may mean that in case of long-term or dramatic climate change, the suitable habitats of halophytic plant species will be seriously affected by climate change (Pigot et al., 2023). This impact may be influenced by the complexity of topography and suitable habitat conditions for halophytic plant species, resulting in different degrees of centroid migration.

5 Conclusions

In this study, a MaxEnt model was used in combination with environmental variables (climate and soil factors) to predict the suitable habitats of six halophytic plant species (*S. salsa*, *S. europaea*, *H. glomeratus*, *H. strobilaceum*, *K. foliatum*, and *H. caspica*) in the arid areas of Northwest China. The results suggested that the distribution of these six halophytic plant species is mainly affected by Bio15, with the most significant influence from the soil factor Na. Compared with the current climate conditions, future climate change may provide opportunities for the expansion of

S. salsa and *K. foliatum*. However, for some halophytic plant species, future climate change may also pose a threat to their survival and growth. As global temperatures continue to increase in the future, *S. salsa* and *K. foliatum* will potentially gain more suitable habitats. However, for other studied halophytic plant species, continued climate change that prevents these species from adapting to changing environmental conditions can lead to a loss in the suitable habitats of plant species. In the future, the potential impact of climate change on the spatial distribution of the suitable habitats for various halophytic plant species would be diverse, with most species shifting toward higher latitudes. This phenomenon is expected to become more pronounced as global warming intensifies in the future. Therefore, future studies should carefully consider the potential impacts of human disturbances and groundwater resources, among other factors. Furthermore, incorporating SDMs will enhance the accuracy of predictions using the MaxEnt model.

Conflict of interest

ZHANG Yuanming is an editorial board member of Journal of Arid Land and was not involved in the editorial review or the decision to publish this article. All authors declare that there are no competing interests.

Acknowledgements

This work was supported by the Third Xinjiang Scientific Expedition Program (2022xjkk1205), the Tianshan Talent Training Program (2023TSYCTD0084), the Science and Technology Major Program of Xinjiang Uygur Autonomous Region (2023A01002), the Young Top Talents of Xinjiang Normal University (XJNUQB2022-29), and the Youth Innovation Promotion Association of the Chinese Academy of Sciences (2020437). We would like to thank the members of our team for their help in the field sample collection.

Author contributions

Conceptualization: YANG Ao, TU Wenqin, ZHUANG Weiwei, YIN Benfeng; Methodology: YANG Ao, TU Wenqin, ZHANG Shujun, ZHANG Xinyu, ZHANG Qing, HUANG Yunjie, HAN Zhili, YANG Ziyue; Formal analysis: YANG Ao, TU Wenqin; Writing - original draft preparation: YANG Ao; Writing - review and editing: ZHUANG Weiwei, YIN Benfeng, ZHANG Yuanming, ZHOU Xiaobing; Funding acquisition: ZHUANG Weiwei, YIN Benfeng; Resources: ZHUANG Weiwei, YIN Benfeng, ZHANG Yuanming; Supervision: ZHUANG Weiwei, YIN Benfeng. All authors approved the manuscript.

References

Abolmaali S M R, Torkesh Esfahani M, Boshri H. 2017. Assessing impacts of climate change on endangered *Kelossia odoratissima* Mozaff species distribution using Generalized Additive Model. Journal of Natural Environment, 70(2): 243–254.

Ahanger M A, Aziz U, Alsahli A A, et al. 2020. Influence of exogenous salicylic acid and nitric oxide on growth, photosynthesis, and ascorbate-glutathione cycle in salt stressed *Vigna angularis*. Biomolecules, 10(1): 42, doi: 10.3390/biom10010042.

Ahmadi F, Mohammadkhani N, Servati M. 2022. Halophytes play important role in phytoremediation of salt-affected soils in the bed of Urmia Lake, Iran. Scientific Reports, 12(1): 12223, doi: 10.1038/s41598-022-16266-4.

An Y, Gao Y, Zhang Y, et al. 2019. Early establishment of *Suaeda salsa* population as affected by soil moisture and salinity: Implications for pioneer species introduction in saline-sodic wetlands in Songnen Plain, China. Ecological Indicators, 107: 105654, doi: 10.1016/j.ecolind.2019.105654.

Ardestani E G, Tarkesh M, Bassiri M, et al. 2015. Potential habitat modeling for reintroduction of three native plant species in central Iran. Journal of Arid Land, 7(3): 381–390.

Barbet-Massin M, Thuiller W, Jiguet F. 2012. The fate of European breeding birds under climate, land-use and dispersal scenarios. Global Change Biology, 18(3): 881–890.

Beaumont L J, Hughes L, Poulsen M. 2005. Predicting species distributions: use of climatic parameters in BIOCLIM and its impact on predictions of species' current and future distributions. Ecological Modelling, 186(2): 251–270.

Bezeng B S, Morales-Castilla I, van der Bank M, et al. 2017. Climate change may reduce the spread of non-native species.

Ecosphere, 8(3): e01694, doi: 10.1002/ecs2.1694.
Brown J L. 2014. SDMtoolbox: a python-based GIS toolkit for landscape genetic, biogeographic and species distribution model analyses. Methods in Ecology and Evolution, 5(7): 694–700.
Cao B, Bai C K, Zhang L L, et al. 2016. Modeling habitat distribution of *Cornus officinalis* with Maxent modeling and fuzzy logics in China. Journal of Plant Ecology, 9(6): 742–751.
Cao C C, Su F L, Song F, et al. 2022. Distribution and disturbance dynamics of habitats suitable for *Suaeda salsa*. Ecological Indicators, 140: 108984, doi: 10.1016/j.ecolind.2022.108984.
Ceballos G, Ehrlich P R, Barnosky A D, et al. 2015. Accelerated modern human–induced species losses: Entering the sixth mass extinction. Science Advances, 1(5): e1400253, doi: 10.1126/sciadv.1400253.
Chen I C, Hill J K, Ohlemüller R, et al. 2011. Rapid range shifts of species associated with high levels of climate warming. Science, 333(6045): 1024–1026.
Chen Q H, Yin Y J, Zhao R, et al. 2019. Incorporating local adaptation into species distribution modeling of *Paeonia mairei*, an endemic plant to China. Frontiers in Plant Science, 10: 1717, doi: 10.3389/fpls.2019.01717.
Collen B, Dulvy N K, Gaston K J, et al. 2016. Clarifying misconceptions of extinction risk assessment with the IUCN Red List. Biology Letters, 12(4): 20150843, doi: 10.1098/rsbl.2015.0843.
Cong M Y, Xu Y Y, Tang L Y, et al. 2020. Predicting the dynamic distribution of *Sphagnum bogs* in China under climate change since the last interglacial period. PLoS ONE, 15(4): e0230969, doi: 10.1371/journal.pone.0230969.
Corlett R T, Westcott D A. 2013. Will plant movements keep up with climate change? Trends in Ecology & Evolution, 28(8): 482–488.
Cutler D R, Edwards T C, Beard K H, et al. 2007. Random forests for classification in ecology. Ecology, 88(11): 2783–2792.
Elith J, Graham C H, Anderson R P, et al. 2006. Novel methods improve prediction of species' distributions from occurrence data. Ecography, 29(2): 129–151.
Elith J, Leathwick J R, Hastie T. 2008. A working guide to boosted regression trees. Journal of Animal Ecology, 77(4): 802–813.
Elith J, Leathwick J R. 2009. Species distribution models: ecological explanation and prediction across space and time. Annual Review of Ecology, Evolution, and Systematics, 40(1): 677–697.
Elith J, Phillips S J, Hastie T, et al. 2011. A statistical explanation of MaxEnt for ecologists. Diversity and Distributions, 17(1): 43–57.
Eswar D, Karuppusamy R, Chellamuthu S. 2021. Drivers of soil salinity and their correlation with climate change. Current Opinion in Environmental Sustainability, 50: 310–318.
Fang X M, Wang Q L, Zhou W M, et al. 2014. Land use effects on soil organic carbon, microbial biomass and microbial activity in Changbai Mountains of Northeast China. Chinese Geographical Science, 24(3): 297–306.
Fang Y Q, Zhang X H, Wei H Y, et al. 2021. Predicting the invasive trend of exotic plants in China based on the ensemble model under climate change: A case for three invasive plants of Asteraceae. Science of the Total Environment, 756: 143841, doi: 10.1016/j.scitotenv.2020.143841.
FAO (Food Agriculture Organization). 2012. Harmonized World Soil Database (version 1.2). FAO, Rome, Italy and IIASA, Laxenburg, Austria. [2023-11-20]. http://webarchive.iiasa.ac.at/Research/LUC/External-World-soil-database/HTML/.
Feeley K J, Bravo-Avila C, Fadrique B, et al. 2020. Climate-driven changes in the composition of New World plant communities. Nature Climate Change, 10(10): 965–970.
Feng X, Park D S, Liang Y, et al. 2019. Collinearity in ecological niche modeling: Confusions and challenges. Ecology and Evolution, 9(18): 10365–10376.
Flowers T J, Colmer T D. 2008. Salinity tolerance in halophytes. New Phytologist, 179(4): 945–963.
Flowers T J, Galal H k, Bromham L. 2010. Evolution of halophytes: multiple origins of salt tolerance in land plants. Functional Plant Biology, 37(7): 604–612.
Foden W, Midgley G F, Hughes G, et al. 2007. A changing climate is eroding the geographical range of the Namib Desert tree *Aloe* through population declines and dispersal lags. Diversity and Distributions, 13(5): 645–653.
Foden W B, Young B E, Akçakaya H R, et al. 2019. Climate change vulnerability assessment of species. WIREs Climate Change, 10(1): e551, doi: 10.1002/wcc.551.
Fourcade Y, Besnard A G, Secondi J. 2018. Paintings predict the distribution of species, or the challenge of selecting environmental predictors and evaluation statistics. Global Ecology and Biogeography, 27(2): 245–256.
Gedan K B, Bertness M D. 2009. Experimental warming causes rapid loss of plant diversity in New England salt marshes. Ecology Letters, 12(8): 842–848.
Gessner U, Naeimi V, Klein I, et al. 2013. The relationship between precipitation anomalies and satellite-derived vegetation

activity in Central Asia. Global and Planetary Change, 110: 74–87.

Gogol-Prokurat M. 2011. Predicting habitat suitability for rare plants at local spatial scales using a species distribution model. Ecological Applications, 21(1): 33–47.

Grant P R, Grant B R. 2002. Unpredictable evolution in a 30-year study of Darwin's finches. Science, 296(5568): 707–711.

Guo J R, Shan C D, Zhang Y F, et al. 2022. Mechanisms of salt tolerance and molecular breeding of salt-tolerant ornamental plants. Frontiers in Plant Science, 13: 854116, doi: 10.3389/fpls.2022.854116.

Hamani A K M, Wang G S, Soothar M K, et al. 2020. Responses of leaf gas exchange attributes, photosynthetic pigments and antioxidant enzymes in NaCl-stressed cotton (*Gossypium hirsutum* L.) seedlings to exogenous glycine betaine and salicylic acid. BMC Plant Biology, 20(1): 434, doi: 10.1186/s12870-020-02624-9.

Hammer E C, Nasr H, Wallander H. 2011. Effects of different organic materials and mineral nutrients on arbuscular mycorrhizal fungal growth in a Mediterranean saline dryland. Soil Biology and Biochemistry, 43(11): 2332–2337.

Han L P, Liu H T, Yu S H, et al. 2013. Potential application of oat for phytoremediation of salt ions in coastal saline-alkali soil. Ecological Engineering, 61: 274–281.

Hasanuzzaman M, Nahar K, Alam M M, et al. 2014. Potential use of halophytes to remediate saline soils. BioMed Research International, 2014: 589341, doi: 10.1155/2014/589341.

Hassani A, Azapagic A, Shokri N. 2021. Global predictions of primary soil salinization under changing climate in the 21st century. Nature communications, 12(1): 6663, doi: 10.1038/s41467-021-26907-3.

Hautier Y, Tilman D, Isbell F, et al. 2015. Anthropogenic environmental changes affect ecosystem stability via biodiversity. Science, 348(6232): 336–340.

Hernandez P A, Graham C H, Master L L, et al. 2006. The effect of sample size and species characteristics on performance of different species distribution modeling methods. Ecography, 29(5): 773–785.

Hirzel A H, Hausser J, Chessel D. 2002. Ecological-niche factor analysis: how to compute habitat-suitability maps without absence data? Ecology, 83(7): 2027–2036.

Hopmans J W, Qureshi A S, Kisekka I, et al. 2021. Critical knowledge gaps and research priorities in global soil salinity. Advances in Agronomy, 169: 1–191.

Hu X G, Jin Y Q, Wang X R, et al. 2015. Predicting impacts of future climate change on the distribution of the widespread conifer *Platycladus orientalis*. PLoS ONE, 10(7): e0132326, doi: 10.1371/journal.pone.0132326.

Huang Z B, Xie L N, Wang H W, et al. 2019. Geographic distribution and impacts of climate change on the suitable habitats of Zingiber species in China. Industrial Crops and Products, 138: 111429, doi: 10.1016/j.indcrop.2019.05.078.

IPBES (Intergovernmental Science-Policy Platform on Biodiversity and Ecosystem Services). 2019. Global Assessment Report on Biodiversity and Ecosystem Services of the Intergovernmental Science-Policy Platform on Biodiversity and Ecosystem Services. In: Brondizio E S, Settele J, Díaz S, et al. Bonn: IPBES Secretariat, 1–1148.

Jesus J M, Danko A S, Fiúza A, et al. 2015. Phytoremediation of salt-affected soils: a review of processes, applicability, and the impact of climate change. Environmental Science and Pollution Research International, 22(9): 6511–6525.

Ju F Y, Pang J L, Sun L Y, et al. 2023. Integrative transcriptomic, metabolomic and physiological analyses revealed the physiological and molecular mechanisms by which potassium regulates the salt tolerance of cotton (*Gossypium hirsutum* L.) roots. Industrial Crops and Products, 193: 116177, doi: 10.1016/j.indcrop.2022.116177.

Khajoei Nasab F, Mehrabian A, Mostafavi H. 2020. Mapping the current and future distributions of *Onosma* species endemic to Iran. Journal of Arid Land, 12(6): 1031–1045.

Khan W D, Tanveer M, Shaukat R, et al. 2020. An overview of salinity tolerance mechanism in plants. In: Hasanuzzaman M, Tanveer M. Salt and Drought Stress Tolerance in Plants: Signaling Networks and Adaptive Mechanisms. Cham: Springer International Publishing, 1–16.

Klein J A, Harte J, Zhao X Q. 2004. Experimental warming causes large and rapid species loss, dampened by simulated grazing, on the Tibetan Plateau. Ecology Letters, 7(12): 1170–1179.

Korell L, Auge H, Chase J M, et al. 2021. Responses of plant diversity to precipitation change are strongest at local spatial scales and in drylands. Nature Communications, 12(1): 2489, doi: 10.1038/s41467-021-22766-0.

Kramer-Schadt S, Niedballa J, Pilgrim J D, et al. 2013. The importance of correcting for sampling bias in MaxEnt species distribution models. Diversity and Distributions, 19(11): 1366–1379.

Lehikoinen A, Virkkala R. 2016. North by north-west: climate change and directions of density shifts in birds. Global Change Biology, 22(3): 1121–1129.

Li B, Wang Z C, Sun Z G, et al. 2005. Resources and sustainable resource exploitation of salinized land in China. Agricultural Research in the Arid Areas, 23(2): 154–158. (in Chinese)

Li J J, Fan G, He Y. 2020. Predicting the current and future distribution of three *Coptis* herbs in China under climate change

conditions, using the MaxEnt model and chemical analysis. Science of the Total Environment, 698: 134141, doi: 10.1016/j.scitotenv.2019.134141.

Li L, Zhang B, Wen A M, et al. 2022. Predicting potential distribution of *Stellera chamaejasme* under global climate change in China. Applied Ecology and Environmental Research, 20(5): 3977–3993.

Li L P, Wang Z H, Zerbe S, et al. 2013. Species richness patterns and water-energy dynamics in the drylands of northwest China. PLoS ONE, 8(6): e66450, doi: 10.1371/journal.pone.0066450.

Liu J Y, Wan J L, Yin X J, et al. 2024. Progress and prospect of developing salt and alkali tolerant rice using hybrid rice technology in China. Plant Breeding, 143(1): 86–95.

Liu L, Bai X G, Jiang Z D. 2019. The generic technology identification of saline–alkali land management and improvement based on social network analysis. Cluster Computing, 22(6): 13167–13176.

Liu L, Guan L L, Zhao H X, et al. 2021. Modeling habitat suitability of *Houttuynia cordata* Thunb (Ceercao) using MaxEnt under climate change in China. Ecological Informatics, 63: 101324, doi: 10.1016/j.ecoinf.2021.101324.

Liu L L, Wang B S. 2021. Protection of halophytes and their uses for cultivation of saline-alkali soil in China. Biology, 10(5): 353, doi: 10.3390/biology10050353.

Liu W S, You J L, Ceng W B, et al. 2018. Prediction of the geographical distribution of *Carex moorcroftii* under global climate change based on MaxEnt model. Chinese Journal of Grassland, 40(5): 43–49. (in Chinese)

Llanes A, Palchetti M V, Vilo C, et al. 2021. Molecular control to salt tolerance mechanisms of woody plants: recent achievements and perspective. Annals of Forest Science, 78(96): 96, doi: 10.1007/s13595-021-01107-7.

Lososová Z, Tichý L, Divíšek J, et al. 2018. Projecting potential future shifts in species composition of European urban plant communities. Diversity and Distributions, 24(6): 765–775.

Lu Y, Zhang B, Li L, et al. 2021a. Negative effects of long-term exposure to salinity, drought, and combined stresses on halophyte *Halogeton glomeratus*. Physiologia Plantarum, 173(4): 2307–2322.

Lu Z Y, Zhai Y P, Meng D R, et al. 2021b. Predicting the potential distribution of wintering Asian Great Bustard (*Otis tarda dybowskii*) in China: Conservation implications. Global Ecology and Conservation, 31(3): e01817, doi: 10.1016/j.gecco.2021.e01817.

Lynn J, Peeva N. 2021. Communications in the IPCC's Sixth Assessment Report cycle. Climatic Change, 169(1–2): 18, doi: 10.1007/s10584-021-03233-7.

Ma B B, Sun J. 2018. Predicting the distribution of *Stipa purpurea* across the Tibetan Plateau via the MaxEnt model. BMC Ecology, 18(1): 10, doi: 10.1186/s12898-018-0165-0.

Ma L G, Yang S T, Simayi Z, et al. 2018. Modeling variations in soil salinity in the oasis of Junggar Basin, China. Land Degradation & Development, 29(3): 551–562.

Mamun M, Kim S, An K. 2018. Distribution pattern prediction of an invasive alien species *largemouth bass* using a maximum entropy model (MaxEnt) in the Korean peninsula. Journal of Asia-Pacific Biodiversity, 11(4): 516–524.

Mantyka-Pringle C S, Visconti P, Di Marco M, et al. 2015. Climate change modifies risk of global biodiversity loss due to land-cover change. Biological Conservation, 187: 103–111.

Mathias A, Chesson P. 2013. Coexistence and evolutionary dynamics mediated by seasonal environmental variation in annual plant communities. Theoretical Population Biology, 84: 56–71.

Melo-Merino S M, Reyes-Bonilla H, Lira-Noriega A. 2020. Ecological niche models and species distribution models in marine environments: A literature review and spatial analysis of evidence. Ecological Modelling, 415: 108837, doi: 10.1016/j.ecolmodel.2019.108837.

Merow C, Smith M J, Silander J A. 2013. A practical guide to MaxEnt for modeling species' distributions: what it does, and why inputs and settings matter. Ecography, 36(10): 1058–1069.

Na X D, Zhou H T, Zang S Y, et al. 2018. Maximum entropy modeling for habitat suitability assessment of red-crowned crane. Ecological Indicators, 91: 439–446.

Nilhan T G, Emre Y A, Osman K. 2008. Soil determinants for distribution of *Halocnemum strobilaceum* Bieb. (Chenopodiaceae) around Lake Tuz, Turkey. Pakistan Journal of Biological Sciences, 11(4): 565–570.

Nouri H, Chavoshi Borujeni S, Nirola R, et al. 2017. Application of green remediation on soil salinity treatment: a review on halophytoremediation. Process Safety and Environmental Protection, 107: 94–107.

Pecl G T, Araújo M B, Bell J D, et al. 2017. Biodiversity redistribution under climate change: Impacts on ecosystems and human well-being. Science, 355(6332): eaai9214, doi: 10.1126/science.aai9214.

Petitpierre B, Mcdougall K, Seipel T, et al. 2016. Will climate change increase the risk of plant invasions into mountains? Ecological Applications, 26(2): 530–544.

Phillips S J, Anderson R P, Schapire R E. 2006. Maximum entropy modeling of species geographic distributions. Ecological

Modelling, 190(3): 231–259.

Phillips S J, Dudík M. 2008. Modeling of species distributions with Maxent: new extensions and a comprehensive evaluation. Ecography, 31(2): 161–175.

Phillips S J, Dudík M, Elith J, et al. 2009. Sample selection bias and presence-only distribution models: implications for background and pseudo-absence data. Ecological Applications, 19(1): 181–197.

Pías B, Matesanz S, Herrero A, et al. 2010. Transgenerational effects of three global change drivers on an endemic mediterranean plant. Oikos, 119: 1435–1444.

Piedallu C, Gégout J, Bruand A, et al. 2011. Mapping soil water holding capacity over large areas to predict potential production of forest stands. Geoderma, 160(3–4): 355–366.

Pigot A L, Merow C, Wilson A, et al. 2023. Abrupt expansion of climate change risks for species globally. Nature Ecology & Evolution, 7(7): 1060–1071.

Pimm S L, Jenkins C N, Abell R, et al. 2014. The biodiversity of species and their rates of extinction, distribution, and protection. Science, 344(6187): 1246752, doi: 10.1126/science.1246752.

Poorter H. 2000. The role of biomass allocation in the growth response of plants to different levels of light, CO_2, nutrients and water: A quantitative review. Australian Journal of Plant Physiology, 27: 595–607.

Popp A, Calvin K, Fujimori S, et al. 2017. Land-use futures in the shared socio-economic pathways. Global Environmental Change, 42: 331–345.

Qin A L, Liu B, Guo Q S, et al. 2017. Maxent modeling for predicting impacts of climate change on the potential distribution of *Thuja sutchuenensis* Franch., an extremely endangered conifer from southwestern China. Global Ecology and Conservation, 10: 139–146.

Qiu Y, Hu Q, Zhang C. 2017. WRF simulation and downscaling of local climate in central Asia. International Journal of Climatology, 37(S1): 513–528.

Qu X X, Huang Z Y, Baskin J M, et al. 2008. Effect of temperature, light and salinity on seed germination and radicle growth of the geographically widespread halophyte shrub *Halocnemum strobilaceum*. Annals of Botany, 101(2): 293–299.

Quevedo-Robledo L, Pucheta E, Ribas-Fernández Y. 2010. Influences of interyear rainfall variability and microhabitat on the germinable seed bank of annual plants in a sandy Monte Desert. Journal of Arid Environments, 74(2): 167–172.

Rabhi M, Hafsi C, Lakhdar A, et al. 2009. Evaluation of the capacity of three halophytes to desalinize their rhizosphere as grown on saline soils under nonleaching conditions. African Journal of Ecology, 47(4): 463–468.

Richman S K, Levine J M, Stefan L, et al. 2020. Asynchronous range shifts drive alpine plant–pollinator interactions and reduce plant fitness. Global Change Biology, 26(5): 3052–3064.

Rocca F D, Milanesi P. 2020. Combining climate, land use change and dispersal to predict the distribution of endangered species with limited vagility. Journal of Biogeography, 47(7): 1427–1438.

Román-Palacios C, Wiens J J. 2020. Recent responses to climate change reveal the drivers of species extinction and survival. Proceedings of the National Academy of Sciences, 117(8): 4211–4217.

Shabala S. 2013. Learning from halophytes: physiological basis and strategies to improve abiotic stress tolerance in crops. Annals of Botany, 112(7): 1209–1221.

Shabala S, Bose J, Hedrich R. 2014. Salt bladders: do they matter? Trends in Plant Science, 19(11): 687–691.

Shao Q, Han N, Ding T L, et al. 2014. SsHKT1;1 is a potassium transporter of the C_3 halophyte *Suaeda salsa* that is involved in salt tolerance. Functional Plant Biology, 41(8): 790–802.

Sheppard C S. 2013. How does selection of climate variables affect predictions of species distributions? A case study of three new weeds in New Zealand. Weed Research, 53(4): 259–268.

Shi X D, Yin Q, Sang Z Y, et al. 2021. Prediction of potentially suitable areas for the introduction of *Magnolia wufengensis* under climate change. Ecological Indicators, 127: 107762, doi: 10.1016/j.ecolind.2021.107762.

Singh A. 2021. Soil salinization management for sustainable development: a review. Journal of Environmental Management, 277: 111383, doi: 10.1016/j.jenvman.2020.111383.

Song G Q, Feng J L, Gong S, et al. 2023. Geographic distribution and impacts of climate change on the suitable habitats of *Rhamnus utilis* Decne in China. BMC Plant Biology, 23(1): 592, doi: 10.1186/s12870-023-04574-4.

Srivastava V, Lafond V, Griess V. 2019. Species distribution models (SDM): applications, benefits and challenges in invasive species management. CAB Reviews Perspectives in Agriculture Veterinary Science Nutrition and Natural Resources, 14: 1–13.

Stockwell D. 1999. The GARP modelling system: problems and solutions to automated spatial prediction. International Journal of Geographical Information Science, 13(2): 143–158.

Sun S X, Zhang Y, Huang D Z, et al. 2020. The effect of climate change on the richness distribution pattern of oaks (*Quercus* L.)

in China. Science of the Total Environment, 744: 140786, doi: 10.1016/j.scitotenv.2020.140786.

Thomas C D, Franco A M A, Hill J K. 2006. Range retractions and extinction in the face of climate warming. Trends in Ecology & Evolution, 21(8): 415–416.

Thomson A M, Calvin K V, Smith S J, et al. 2011. RCP4.5: A pathway for stabilization of radiative forcing by 2100. Climatic Change, 109: 77, doi: 10.1007/s10584-011-0151-4.

Tu W Q, Xiong Q L, Qiu X P, et al. 2021. Dynamics of invasive alien plant species in China under climate change scenarios. Ecological Indicators, 129: 107919, doi: 10.1016/j.ecolind.2021.107919.

van Zelm E, Zhang Y X, Testerink C. 2020. Salt tolerance mechanisms of plants. Annual Review of Plant Biology, 71(1): 403–433.

Vitt P, Havens K, Kramer A T, et al. 2010. Assisted migration of plants: changes in latitudes, changes in attitudes. Biological Conservation, 143(1): 18–27.

Wang F, Yuan X Z, Sun Y J, et al. 2024. Species distribution modeling based on MaxEnt to inform biodiversity conservation in the central urban area of Chongqing Municipality. Ecological Indicators, 158: 111491, doi: 10.1016/j.ecolind.2023.111491.

Wang H F, Kong L, Gao R, et al. 2019. Germination biology of dimorphic seeds of the annual halophyte common seepweed (*Suaeda glauca*). Weed Science, 68(2): 143–150.

Wang J R, Hawkins C D B, Letchford T. 1998. Photosynthesis, water and nitrogen use efficiencies of four paper birch (*Betula papyrifera*) populations grown under different soil moisture and nutrient regimes. Forest Ecology and Management, 112(3): 233–244.

Wang S, Sun L, Rao M P N, et al. 2021. Insights into the microbial diversity in saline-alkaline soils of China. In: Egamberdieva D, Birkeland N K, Li W J, et al. Microbial Communities and Their Interactions in the Extreme Environment. Singapore: Springer, 17–41.

Wang Y G, Deng C Y, Liu Y, et al. 2018. Identifying change in spatial accumulation of soil salinity in an inland river watershed, China. Science of the Total Environment, 621: 177–185.

Wang Y Y, Wang S Q, Zhao Z Y, et al. 2023. Progress of euhalophyte adaptation to arid areas to remediate salinized soil. Agriculture, 13(3): 704, doi: 10.3390/agriculture13030704.

Warren D L, Glor R E, Turelli M. 2010. ENMTools: a toolbox for comparative studies of environmental niche models. Ecography, 33(3): 607–611.

Warren D L, Wright A N, Seifert S N, et al. 2014. Incorporating model complexity and spatial sampling bias into ecological niche models of climate change risks faced by 90 California vertebrate species of concern. Diversity and Distributions, 20(3): 334–343.

Warren R, Price J, Graham E, et al. 2018. The projected effect on insects, vertebrates, and plants of limiting global warming to 1.5°C rather than 2°C. Science, 360(6390): 791–795.

Wei S G, Dai Y J, Liu B Y, et al. 2013. A China data set of soil properties for land surface modeling. Journal of Advances in Modeling Earth Systems, 5(2): 212–224.

Wu T W, Song L C, Li W P, et al. 2014. An overview of BCC climate system model development and application for climate change studies. Journal of Meteorological Research, 28(1): 34–56.

Wu T W, Lu Y X, Fang Y J, et al. 2019. The Beijing Climate Center Climate System Model (BCC-CSM): the main progress from CMIP5 to CMIP6. Geoscientific Model Development, 12(4): 1573–1600.

Xian X Q, Zhao H X, Guo J Y, et al. 2022. Estimation of the potential geographical distribution of a new potato pest (*Schrankia costaestrigalis*) in China under climate change. Journal of Integrative Agriculture, 22(8): 2441–2455.

Xiong Q L, Xiao Y, Halmy M W A, et al. 2019. Monitoring the impact of climate change and human activities on grassland vegetation dynamics in the northeastern Qinghai-Tibet Plateau of China during 2000–2015. Journal of Arid Land, 11(5): 637–651.

Xiong Q L, Luo X J, Liang P H, et al. 2020. Fire from policy, human interventions, or biophysical factors? temporal–spatial patterns of forest fire in southwestern China. Forest Ecology and Management, 474: 118381, doi: 10.1016/j.foreco.2020.118381.

Yang B, Qin S Y, Xu W S, et al. 2020. Gap analysis of giant panda conservation as an example for planning China's national park system. Current Biology, 30(7): 1287–1291.e2.

Yang H, Jiang Z H, Li L. 2016. Biases and improvements in three dynamical downscaling climate simulations over China. Climate Dynamics, 47(9): 3235–3251.

Yang Z B, Bai Y, Alatalo J M, et al. 2021. Spatio-temporal variation in potential habitats for rare and endangered plants and habitat conservation based on the maximum entropy model. Science of the Total Environment, 784: 147080, doi: 10.1016/j.scitotenv.2021.147080.

Ye P C, Zhang G F, Zhao X, et al. 2021. Potential geographical distribution and environmental explanations of rare and endangered plant species through combined modeling: a case study of Northwest Yunnan, China. Ecology and Evolution, 11(19): 13052–13067.

Yi Y J, Cheng X, Yang Z F, et al. 2016. Maxent modeling for predicting the potential distribution of endangered medicinal plant (*H. riparia* Lour) in Yunnan, China. Ecological Engineering, 92: 260–269.

Yilmaz H, Yilmaz O Y, Akyüz Y F. 2017. Determining the factors affecting the distribution of *Muscari latifolium*, an endemic plant of Turkey, and a mapping species distribution model. Ecology and Evolution, 7(4): 1112–1124.

Yin B F, Zhang Y M, Zhang H X, et al. 2023. Phylogeographic structure of *Syntrichia caninervis* Mitt, a xerophytic moss, highlights the expanded during glacial period. Journal of Plant Ecology, 16(2): rtac057, doi: 10.1093/jpe/rtac057.

Yuan J, Wang X Q, Zhao Y, et al. 2020. Genetic basis and identification of candidate genes for salt tolerance in rice by GWAS. Scientific Reports, 10(1): 9958, doi:10.1038/s41598-020-66604-7.

Zhang H, Irving L J, Tian Y, et al. 2012. Influence of salinity and temperature on seed germination rate and the hydrotime model parameters for the halophyte, *Chloris virgata*, and the glycophyte, *Digitaria sanguinalis*. South African Journal of Botany, 78: 203–210.

Zhang H, Wang X P, Zhang Y F, et al. 2015. Responses of plant growth of different life forms to rainfall amount changes in an arid desert area. Chinese Journal of Ecology, 34: 1847–1853. (in Chinese)

Zhang H, Zhao H X. 2021. Study on rare and endangered plants under climate: Maxent modeling for identifying hot spots in Northwest China. CERNE, 27(1): e-102667, doi: 10.1590/01047760202127012667.

Zhang J J, Jiang F, Li G Y, et al. 2019. Maxent modeling for predicting the spatial distribution of three raptors in the Sanjiangyuan National Park, China. Ecology and Evolution, 9(11): 6643–6654.

Zhang J L, Shi H Z. 2013. Physiological and molecular mechanisms of plant salt tolerance. Photosynthesis Research, 115(1): 1–22.

Zhang Y, Tang J S, Ren G, et al. 2021. Global potential distribution prediction of *Xanthium italicum* based on Maxent model. Scientific Reports, 11(1): 16545, doi: 10.1038/s41598-021-96041-z.

Zhao S, Liu X, Banerjee S, et al. 2024. Continuous planting of euhalophyte *Suaeda salsa* enhances microbial diversity and multifunctionality of saline soil. Applied and Environmental Microbiology, 90(4): e02355-23, doi: 10.1128/aem.02355-23.

Zhao Y, Li Y Y, Wang J, et al. 2016. Buried straw layer plus plastic mulching reduces soil salinity and increases sunflower yield in saline soils. Soil and Tillage Research, 155: 363–370.

Zhao Y, Deng X W, Xiang W H, et al. 2021. Predicting potential suitable habitats of Chinese fir under current and future climatic scenarios based on Maxent model. Ecological Informatics, 64: 101393, doi: 10.1016/j.ecoinf.2021.101393.

Zhou H P, Shi H F, Yang Y Q, et al. 2024. Insights into plant salt stress signaling and tolerance. Journal of Genetics and Genomics, 51(1): 16–34.

Appendix

Table S1 Description of the 40 environmental variables in this study

Variable	Definition	Unit	Variable	Definition	Unit
Bio1	Annual mean temperature	°C	Slope	Slope	°
Bio2	Mean diurnal range	°C	Aspect	Aspect index	°
Bio3	Isothermality ((Bio2/Bio7)×100)	-	AN	Available nitrogen	mg/kg
Bio4	Temperature seasonality	°C	AP	Available phosphorus	mg/kg
Bio5	Maximum temperature of the warmest month	°C	AK	Available potassium	mg/kg
Bio6	Minimum temperature of the coldest month	°C	BD	Soil bulk density	g/cm^3
Bio7	Temperature annual range	°C	BS	Soil base saturation	%
Bio8	Mean temperature of the wettest quarter	°C	SOM	Soil organic matter	%
Bio9	Mean temperature of the driest quarter	°C	pH	Acidity and basicity	-
Bio10	Mean temperature of the warmest quarter	°C	SOC	Soil organic carbon	%
Bio11	Mean temperature of the coldest quarter	°C	CEC_SOIL	Cation exchange capacity	cmol/kg
Bio12	Annual precipitation	mm	SILT	Silt content	%
Bio13	Precipitation of the wettest month	mm	CLAY	Clay content	%
Bio14	Precipitation of the driest month	mm	SAND	Sand content	%
Bio15	Precipitation seasonality (coefficient of variation)	mm	ECE	Electrical conductivity	dS/m
Bio16	Precipitation of the wettest quarter	mm	TEB	Soil exchangeable base	cmol/kg
Bio17	Precipitation of the driest quarter	mm	ESP	Soil sodicity	%
Bio18	Precipitation of the warmest quarter	mm	POR	Porosity	%
Bio19	Precipitation of the coldest quarter	mm	Na	Exchangeable Na^+	cmol/kg
DEM	Altitude	m	$CACO_3$	Soil calcium carbonate	%

Note: - indicates dimensionless.

Table S2 Contribution rates of the selected 16 environmental variables to the distribution of six halophytic plant species based on the maximum entropy (MaxEnt) model

Variable	Contribution rate (%)						
	S. salsa	*S. europaea*	*H. glomeratus*	*H. strobilaceum*	*K. foliatum*	*H. caspica*	Average
Na	31.40	28.40	5.00	4.60	9.70	14.50	11.68
AN	7.80	5.30	6.90	8.80	4.50	3.00	6.87
pH	7.40	10.50	1.60	0.30	6.20	4.20	3.33
BS	2.50	10.00	2.90	3.40	10.10	0.50	3.72
TEB	2.40	2.30	3.80	6.70	2.60	1.90	4.02
POR	0.90	0.10	0.90	0.60	3.10	2.90	1.53
ECE	0.90	0.80	3.40	2.40	2.40	9.10	3.47
$CaCO_3$	6.10	1.90	2.00	2.50	5.30	1.10	3.38
CEC_SOIL	3.20	7.80	5.60	11.50	5.90	4.20	6.08
Bio2	3.20	0.30	2.60	1.80	5.70	5.90	3.43
Bio7	3.70	3.10	1.50	4.00	1.70	8.80	3.72
Bio10	6.80	5.10	0.20	5.50	9.90	1.00	4.90
Bio11	3.60	2.30	0.60	1.10	5.80	5.10	2.83
Bio15	1.70	9.40	44.00	32.00	2.00	23.40	23.15
Bio18	8.80	10.40	17.40	11.10	19.60	10.70	13.20
Bio19	9.70	2.10	1.60	3.50	5.40	3.70	4.62

Table S3 Suitable habitat ranges of the selected 16 environmental variables for the six halophytic plant species based on the retention of environmental factor response curves

Variable	*S. salsa*	*S. europaea*	*H. glomeratus*
Na (cmol/kg)	0.11–0.17	0.11–0.17	0.10–0.18
AN (mg/kg)	94.43–95.10	39.77–103.10	41.11–109.77
pH	8.03–8.45	8.12–8.49	8.24–9.82
BS (%)	99.85–100.00	99.88–100.00	99.80–100.00
TEB (cmol/kg)	40.81–40.89	21.15–68.20	1.60–17.96
POR (%)	43.32–50.14	47.69–52.70	47.11–52.26
ECE (dS/m)	30.41–42.80	15.30–42.80	9.97–42.80
$CaCO_3$ (%)	4.70–15.53	0.62–19.67	0.80–29.50
CEC_SOIL (cmol/kg)	43.48–87.00	1.00–2.31	1.00–1.79
Bio2 (℃)	10.10–13.53	10.67–14.51	10.10–13.64
Bio7 (℃)	39.07–46.93	41.60–48.91	41.36–47.72
Bio10 (℃)	19.40–23.94	20.17–25.21	20.97–32.56
Bio11 (℃)	–7.96–4.58	–9.92– –2.17	–12.42– –0.61
Bio15 (mm)	82.27–111.27	12.07–72.35	23.26–70.13
Bio18 (mm)	86.29–270.86	41.66–140.86	39.36–95.47
Bio19 (mm)	3.28–69.00	24.21–66.00	15.88–62.00
Environmental variable	*H. strobilaceum*	*K. foliatum*	*H. caspica*
Na (cmol/kg)	0.09–0.17	0.11–0.17	0.12–0.17
AN (mg/kg)	49.11–107.10	31.78–102.43	35.11–109.10
pH	8.07–8.47	8.15–8.57	8.18–8.60
BS (%)	90.00–100.00	99.80–100.00	99.80–100.00
TEB (cmol/kg)	29.55–68.20	19.43–57.30	20.27–47.64
POR (%)	45.99–52.14	45.99–52.39	47.51–52.84
ECE (dS/m)	17.20–42.80	6.92–42.80	28.78–42.80
$CaCO_3$ (%)	1.51–29.50	1.51–18.96	1.09–29.50
CEC_SOIL (cmol/kg)	1.00–1.69	35.33–87.00	1.00–1.89
Bio2 (℃)	10.10–13.65	10.89–14.24	10.52–14.13
Bio7 (℃)	42.05–49.05	40.55–47.22	40.88–46.71
Bio10 (℃)	21.87–30.76	–10.33– –1.82	20.67–25.65
Bio11 (℃)	–6.77–1.14	–27.48–4.74	–8.45–1.23
Bio15 (mm)	23.26–68.34	37.17–80.05	23.22–76.41
Bio18 (mm)	30.18–96.70	45.98–169.6	35.50–116.14
Bio19 (mm)	3.22–66.00	2.64–7.14	5.95–63.00